Submitted to Journal of Chemical Physics

UCRL-19559
Preprint

c.2

RECEIVED
LAWRENCE
RADIATION LABORATORY
JUN 2 1970
LIBRARY AND
DOCUMENTS SECTION

MÖSSBAUER SPECTROSCOPY OF GOLD COMPOUNDS

Marjorie O. Faltens and D. A. Shirley

February 1970

AEC Contract No. W-7405-eng-48

TWO-WEEK LOAN COPY

This is a Library Circulating Copy which may be borrowed for two weeks. For a personal retention copy, call Tech. Info. Division, Ext. 5545

UCRL-19559

LAWRENCE RADIATION LABORATORY
UNIVERSITY of CALIFORNIA BERKELEY

DISCLAIMER

This document was prepared as an account of work sponsored by the United States Government. While this document is believed to contain correct information, neither the United States Government nor any agency thereof, nor the Regents of the University of California, nor any of their employees, makes any warranty, express or implied, or assumes any legal responsibility for the accuracy, completeness, or usefulness of any information, apparatus, product, or process disclosed, or represents that its use would not infringe privately owned rights. Reference herein to any specific commercial product, process, or service by its trade name, trademark, manufacturer, or otherwise, does not necessarily constitute or imply its endorsement, recommendation, or favoring by the United States Government or any agency thereof, or the Regents of the University of California. The views and opinions of authors expressed herein do not necessarily state or reflect those of the United States Government or any agency thereof or the Regents of the University of California.

MÖSSBAUER SPECTROSCOPY OF GOLD COMPOUNDS*

Marjorie O. Faltens and D. A. Shirley

Department of Chemistry
and Lawrence Radiation Laboratory
University of California
Berkeley, California 94720

February 1970

ABSTRACT

Mössbauer spectra at 4.2°K were taken with ^{197}Au in several aurous and auric compounds. For each oxidation state a linear correlation was observed between the isomer shift (IS) and the quadrupole splitting (QS). Both the IS and QS varied over wide ranges in both auric and aurous compounds. Neither IS nor QS alone could be used to determine the oxidation state, but together they appear to determine it uniquely. The results for linear aurous and square-planar auric complexes are interpreted in terms of 6s6p and $5d6s6p^2$ hybridization, respectively, with varying degrees of ionic character. Attempts to interpret the results quantitatively in terms of the atomic parameters $\psi^2(0)$ and $\langle r^{-3} \rangle$ were only partially successful: it was not possible to reproduce the large experimental values for $\langle r^{-3} \rangle_{6p}$ using free atom theory. The nuclear factor was determined as $\delta R/R = +(2.5 \pm 0.6)$ using the simple hybridization model.

I. INTRODUCTION

Monoisotopic Au-197 possesses one of the best resonances for chemical applications of Mössbauer spectroscopy. Although the natural linewidth of the 77-keV resonance is about 50 times that of ^{57}Fe, the ranges of both isomer shifts and quadrupole coupling constants are also much larger in ^{197}Au than in ^{57}Fe, thus rendering the gold resonance of nearly equal value for structural chemical work. Relatively little application of the ^{197}Au resonance to chemical problems has been made until now, however.[1,2] The present work was carried out to test further the feasibility of such application and to establish the systematic relationships of the Mössbauer spectra to chemical structure.

Section II is a description of experimental procedures. Results are given in Section III. In Section IV these results are intercompared and correlations are made. A simple interpretation is given in Section V.

II. EXPERIMENTAL

A. Source

Sources of ^{197}Pt in Pt metal were made by neutron irradiation of 10 mg discs of metallic Pt enriched to 65% in ^{196}Pt. These discs were used as received from the reactor, without further treatment. A single disc could be used repeatedly. The decay scheme[3] of 18-hour ^{197}Pt is shown in Fig. 1. Absorbers consisted of (monoiostopic) ^{197}Au in gold compounds.

B. Preparation of Absorber Samples

Most of the absorber samples were prepared in this Laboratory. Some of the less stable gold compounds were made only a few minutes before the experiments were performed, to avoid excessive decomposition. Once the absorber samples were in the cryostat, which was maintained at 4.2°K in an inert atmosphere of helium exchange gas at ∿ 2 Torr, the decomposition process was virtually arrested. About a half gram of gold absorber was constrained to a disc of 2 cm^2 area in a plastic sample holder. Some of the more unstable compounds showed slight signs of decomposition on the surfaces of this disc. However in each such case only a small percentage of the total effective sample was thus affected, with no observable effect on the Mössbauer spectrum.

The methods of absorber preparation are summarized in the flow chart in Fig. 2 and are described briefly below. The marginal stability of most of these compounds and the unreliability of commercial preparations made this the most sensitive aspect of the research reported here. More details of the syntheses are given elsewhere.[4] Many of the compounds are vividly colored, thus facilitating their preparation and identification. Most of the compounds were characterized by chemical analysis.

In preparing gold samples for spectroscopy one can employ the fact that gold is a member of a small group of metals which form metal halides having the following order of stability:

Iodide > Bromide > Chloride > Fluoride.

Most metals have the reversed order of stability. In general, a given gold(III) compound is more stable than the corresponding gold(I) compound,

the latter usually having a tendency to disproportionate into the auric compound plus elemental gold. Gold forms covalent bonds in great preference to ionic bonds and forms complexes apparently without exception, to increase the coordination numbers from one to two in the aurous state and from three to four in the auric state.

The compounds used in this work were prepared as follows (cf. Fig. 2):

1. $[BrF_2]^+[AuF_4]^-$ was prepared by reacting gold metal with liquid BrF_3.[5] Since BrF_3 is both highly corrosive and extremely toxic, the preparation was made in a monel vacuum system. The transfer of this dull yellow, very hygroscopic compound from the reaction vessel into the absorber holder was done in a dry box to avoid forming the black hydroxide (oxide) of gold. Teflon absorber holders were used for this compound. No chemical analysis was performed on this compound.

2. Orange AuF_3 was made by heating $[BrF_2]^+[AuF_4]^-$ to 50°C and removing the excess BrF_3 in a cold finger. AuF_3, also highly hygroscopic, was treated with the same precautions used for $[BrF_2]^+[AuF_4]^-$. A chemical analysis disclosed a gold-to-fluorine molar ratio of 1.0/3.0.

3. Chlorauric acid, $HAuCl_4$, was formed by dissolving gold metal in aqua regia. It is a reasonably stable orange-colored compound.

4. Chlorauric acid was converted to the dark reddish-brown $AuCl_3$ by heating the acid to 175°C in a tube furnace in an atmosphere of dry chlorine gas. Atmospheric moisture can decompose $AuCl_3$.

5. AuCl was made from $AuCl_3$ by heating the latter in a tube furnace to a temperature of 235°C in an atmosphere of dry HCl gas. AuCl can be distinguished from the dark reddish brown $AuCl_3$ by its light yellow color. A typical chemical analysis gave a chlorine-to-gold molar ratio of 1.05/1.00.

6. $Cs_2Au(I)Au(III)Cl_6$ was precipitated from an acid solution of CsCl and AuCl.[6] $Cs_2Au(I)Au(III)Cl_6$ is a black solid which contains gold in two oxidation states.

7. Both $NaAuCl_4$ and $KAuCl_4$ were purchased from Alfa Inorganics. $NaAuCl_4$ is a golden yellow salt and $KAuCl_4$ is a bright yellow salt.

8. $AuBr_3$ was prepared by stirring Au powder with liquid bromine. The black product had a bromine-to-gold molar ratio of 2.96/1.00.

9. AuBr, a pale yellow substance, was prepared by heating $AuBr_3$ in a tube furnace to 100°C in a stream of dry argon gas. At about 115°C, AuBr will decompose into its elements. The compound was analyzed as having a gold-to-bromine molar ratio of 1.006/1.000.

10. $KAuBr_4$ was synthesized by dissolving gold powder in an aqueous solution of Br_2 and KBr.[7] This dark reddish-brown compound was recrystallized from methanol. The chemical analysis gave the following molar ratios: K/Au/Br = 1.02/1.00/3.97.

11. AuI_3 is an extremely unstable compound which decomposes at room temperature. We attempted to synthesize it by slowly pouring a cold, dilute aqueous solution of $HAuCl_4$ into an aqueous solution of KI.[8] The precipitate, which was initially brown, turned slowly to a green clay-like substance on standing. The chemical analysis gave an iodine-to-gold ratio of 2.8/1.0 We believe that the substance was essentially converted to AuI and elemental iodine by the time we were able to perform the Mössbauer experiments.

12. AuI is very easy to prepare. This yellow compound was precipitated by slowly pouring a dilute aqueous solution of KI into an equivalent amount of a dilute aqueous solution of $HAuCl_4$ (cf. AuI_3 above).

This finely divided substance, which decomposes when dried, had a green tinge and gave a different iodine-to-gold molar ratio than did the above preparation for AuI_3: I/Au = 1.05/1.00.

13. $KAu(CN)_2$, a colorless crystalline substance, was synthesized from elemental gold by the cyanide process used by gold miners. Gold was dissolved in a dilute aqueous solution of KCN in the presence of atmospheric oxygen. Five grams of 30 mesh gold powder could be dissolved overnight when stirred vigorously in a dilute KCN solution. We bubbled a thin stream of oxygen through the solution.

14. AuCN, a sparingly soluble bright yellow substance, was made by heating an acidic solution of $KAu(CN)_2$ to 50°C.

15. The trans-dicyanodihaloaurate(III) complexes were formed by dissolving $KAu(CN)_2$ in a solution of 100 cc water and 30 cc methanol and adding the appropriate halogen.[9] To make $KAu(CN)_2Cl_2$, Cl_2 gas was bubbled through the solution. Methyl alcohol solutions of liquid bromine and elemental iodine were added to $KAu(CN)_2$ to make $KAu(CN)_2Br_2$ and $KAu(CN)_2I_2$, respectively. The chemical analyses of the dicyanodihaloaurate(III) compounds gave the ratios:

K/Au/CN/Cl = 1.02/1.00/1.99/1.99

K/Au/CN/Br = 1.03/1.00/2.05/1.98

K/Au/CN/I = 1.02/1.00/2.04/2.05 .

The chloride salt is pale yellow, the bromide is bright yellow and the iodide is deep reddish-brown. $KAu(CN)_2I_2$ is the least stable of the three congeners.

16. $KAu(CN)_4$, a colorless stable gold compound, was prepared by treating $KAu(CN)_2Br_2$ with KCN. The $KAu(CN)_4$ solution was decanted to

separate it from KBr crystals which came out of solution at high concentrations. The chemical analysis gave: K/Au/CN = 1.08/1.00/4.02.

17. $Na_3Au(S_2O_3)_2$ was synthesized by neutralizing $HAuCl_4$ with NaOH, then reacting the resulting solution with $Na_2S_2O_3$ to give the colorless $Na_3Au(S_2O_3)_2$ salt.[10] Care was taken to pour the thiosulfate solution into the gold hydroxide solution, to avoid precipitating an insoluble gold sulfide.

18. Au_2O_3 was purchased from Alpha Inorganics as a brown powder.

19. $[(C_2H_5)_4N]^+[AuS_4C_4(CN)_4]^-$ was kindly provided by Dr. N. Edelstein. It is a reddish-brown crystalline substance.

20. The three gold sulfides were all black, finely divided substances which were amorphous, according to their x-ray patterns. Only Au_2S_2, $(Au{\cdot}AuS_2)$, showed faint lines in its powder pattern.

Au_2S was precipitated from an acid solution of $KAu(CN)_2$ by bubbling in H_2S. This initially dark reddish-brown precipitate turns steel-gray. The chemical analysis yielded the gold-to-sulfur molar ratio 2.04/1.00.

21. Au_2S_3 was prepared by passing H_2S through a solution of chlorauric acid in anhydrous ether. A chemical analysis yielded a gold-to-sulfur molar ratio of 1.00/1.65, a little high in sulfur. This may have been due to occluded H_2S.

22. Au_2S_2 was made by reacting H_2S with an aqueous solution of auric chloride. The chemical analysis gave a gold-to-sulfur ratio of 1.000/1.007.

C. Apparatus

A Doppler velocity, which was controlled by a closed-loop linear-drive system, was imposed on the absorber. The drive system consisted of a loudspeaker drive coil, a velocity transducer, and electronic circuitry which is described briefly below and more completely elsewhere.[11] The gamma rays which were transmitted through the absorber sample (or absorbed and retransmitted) were detected by a 1-inch-thick NaI(Tl) scintillation counter. Pulses corresponding to the 77-keV peak were selected by a single-channel analyzer. The output (logic) pulses were sent into a multichannel analyzer operating in the multiscalar mode.

In the linear-drive amplifier, a 20-kc tuning-fork oscillator was used to synchronize the multiscalar start-advance pulses with the waveform of the drive coil output. The 400 channels of the multiscalar were sequentially addressed by a 10 kc pulse derived from the 20 kc oscillator. A 10 kc pulse advance frequency was further divided by 400 to produce a 25-cps square-wave which was used to reset the address of the multiscalar analyzer after all 400 channels have been scanned. A 25 cps triangular wave was produced by integrating the above square wave which had first been amplitude-stabilized by a precision squaring circuit. This frequency source effectively synchronized the channel numbers and the instantaneous velocity of the source.

Within the drive unit, the 25-cps reference triangle wave form was fed into the closed-loop negative feedback drive system to drive the loudspeaker coil. An additional small parabolic correction term to the triangle wave was used to further linearize the velocity.[11] This parabolic wave was obtained by integrating the reference triangle wave and

was therefore automatically synchronized with the system. When the feedback drive system was properly balanced, the deviation from linearity of the velocity wave form was less than 1% over 90% of the velocity range. Even so, combining the "up" and "down" sides of the triangular velocity wave would have resulted in lower resolution, so they were analyzed separately. A schematic diagram of the circuit is given in Fig. 3. Each time a spectrum was run the velocity waveform was calibrated before removing the sample. This was accomplished by converting the voltage output of the transducer to a corresponding frequency using a modified VIDAR 260B voltage-to-frequency converter. The frequency-to-velocity conversion for each transducer was established by obtaining the well-known six-line Mössbauer spectrum of ^{57}Fe and determining the separation (in voltage) of the two outer Zeeman components. A separation of 1.066 ± 0.004 cm/sec was obtained by an absolute laser interferometer calibration[12] at room temperature. Preston, Hanna, and Heberle[13] had previously determined the splitting of the outer-Zeeman components at room temperature and 4.2°K as 1.061 cm/sec and 1.089 cm/sec respectively. Hanna's values were used to convert the laser-calibrated room temperature value to one applicable at 4.2° K. This separation is 1.094 cm/sec.

Data analysis was accomplished with FLOR, a computer program for the CDC 6600 that fits Lorentz curves to a spectrum. This program is written as a subroutine to VARMIT, a least-squares fitting program. A report by Davidon[14] gives the mathematical details of the method. For many gold compounds, the quadrupole splittings are not great enough compared to the linewidths to give well-resolved component lines. FLOR

facilitates the resolution of these lines and determines their intensities, linewidths and line positions. There are provisions in FLOR for setting the value of any parameter to a fixed constant and for imposing linear constraints among the parameters as governed by the Hamiltonian.

FLOR computes the root-mean-square uncertainties, RMSU, for each parameter. The RMSU is a measure of the statistical error and is equal to the square root of the diagonal elements of the H (inverse Hessian) matrix which is generated by VARMIT. For Mössbauer experiments, with good statistical accuracies, the RMSU values are almost identical to the standard deviation values as determined by the method of maximum likelihood (Poisson Statistics). Unfortunately, these RMSU values are small for the linewidths and line positions and often give little indication of the reproducibility of the results. We therefore report the probable error,

$$pe = 0.675 \left[\frac{1}{M} \sum_{i=1}^{M} (x_i - \bar{x})^2 \right]^{1/2} \qquad (1)$$

where M is the number of Mössbauer experiments, $\bar{x}$ is the average of the parameters and the x_i's are the individual measurements. The pe is the 50% confidence limit. That is, given a single additional experiment, there is a 50% chance that its results will be within the pe of the previous identical experiment.

III. EXPERIMENTAL RESULTS

The spectra are presented below for groups of compounds that are logically considered together. Where relevent, comparisons are made with other experiments. Unless otherwise stated, the spectra were fitted with two Lorentz curves of equal linewidths and intensities. Several of the compounds had slightly asymmetric spectra which could have several possible causes: oriented crystallites, chemically inequivalent gold atoms, or the Gol'danskii effect. Some structural information is included here, to facilitate understanding of the spectra. More detailed crystal structure information, with references, is given elsewhere.[4]

A. AuCl, AuBr, AuI

The Mössbauer spectra of the aurous halides AuCl, AuBr, and AuI are shown in Fig. 4. The coordination of the gold atom in AuI[15] is depicted in Fig. 5. It is assumed that AuCl and AuBr have similar structures namely long zig-zag polymers with linear coordination at the gold atom. No crystallographic structural determination has been done on AuCl or AuBr, which are both unstable compounds. Figure 4 includes the spectrum of AuI_3, for reasons explained in Sec. III.E. below.

Shirley, Grant, and Keller[2] did Mössbauer experiments on these aurous halides earlier, while Machmer[16] and Machmer et al.[17] have observed pure quadrupole spectra of ^{197}Au in AuCl and AuI. All the results are set out for comparison in Table I. The results of Ref. 2 are in agreement with those of this work, within experimental error. However, the quadrupole splitting results of Ref. 17 were over 10% lower for AuCl and those of Ref. 16 were about 3% higher for AuI. The ambient temperatures of the

samples in this work was substantially lower than those temperatures used in Refs. 16 and 17, but this probably will not explain the discrepancies. With these unstable aurous halides, there is always the possibility of decomposition. We feel, however, that once in our vacuum cryostat at 4.2°K and inert atmosphere of helium-exchange gas, our absorbers probably did not decompose appreciably during an experiment, and we have no satisfactory explanation for the disagreement.

B. $Na_3Au(S_2O_3)_2 \cdot 2H_2O$

The spectrum of $Na_3Au(S_2O_3)_2 \cdot 2H_2O$ is shown in Fig. 6. This compound is essentially linearly bonded at the gold atom, as illustrated in Fig. 7.[18] The tentative Au-S interatomic distance in this compound is 2.28 Å. The linewidth, 0.317(0.020) cm/sec, is large due partly to the thick absorber sample we used. The gold content of the sample has not been determined.

C. AuCN, $KAu(CN)_2$

Among those compounds included in this work, the gold cyanides have the most positive isomer shift and largest quadrupole splitting. The Mössbauer spectra of AuCN and $KAu(CN)_2$ are given in Fig. 8. The crystal structure of AuCN is not known due to the difficulty of preparing single crystals. A powder pattern study has been made of this compound, but the results are ambiguous because of the difficulty of differentiating between the carbon and nitrogen atoms. The AuCN structure[19,20] probably involves both a nitrogen and a carbon bond to the gold atom to form a

long polymer:

$$\text{Au - C - N - Au - C - N}$$
$$|\leftarrow 5.09\ \text{Å} \rightarrow|$$

This may be a zig-zag polymer[21] with a bend at either the carbon or nitrogen bonds. $KAu(CN)_2$ single crystals are relatively easy to grow, and x-ray analysis shows that the structure has linear units of cyanide-gold-cyanide aggregates. By means of infrared spectroscopy[22] it has been determined that the carbon atoms are directly bonded to the gold atoms as is illustrated in Fig. 9.[23]

D. AuF_3 and $[BrF_2]^+[AuF_4]^-$

The Mössbauer spectra for the auric halides are not as well resolved as for the aurous halides. The spectra of the auric fluorides, AuF_3 and $[BrF_2]^+[AuF_4]^-$, are illustrated in Fig. 10. The lines are symmetrical and partially resolved. Both gold fluorides are extremely unstable and showed signs of some decomposition even while in the cryostat. Several experiments were made on the same samples by changing the Doppler velocity range and readjusting the linear drive amplifier but not disturbing the absorber which was in the cryostat. The quality and resolution of the Mössbauer spectra deteriorated slightly from one experiment to the next. The colors of the absorbers turned slightly dark at the surfaces which were in contact with the absorber holder, indicating that some gold hydroxide probably had been formed. The first experiments on both AuF_3 and $[AuF_4]^-$ gave the best spectra. Roberts et al.[1] also did Mössbauer

experiments on these gold fluorides. Their results are listed with ours in Table II. The isomer shift results for AuF_3 are in agreement, but we expected closer agreement for the $[AuF_4]^-$ results. This difference may be due to the different cations. Roberts et al. did not report quadrupole splittings for the gold fluorides. The coordination[24] of the gold atom in AuF_3 is depicted in Fig. 11.

E. $AuCl_3$, $NaAuCl_4$, $KAuCl_4$, $AuBr_3$, $KAuBr_4$

The auric halides had very small quadrupole coupling constants (Fig. 12). The order of stability for four of these compounds is approximately as follows, starting with the least stable: $AuCl_3$; $KAuCl_4$ and $NaAuCl_4$; $KAuBr_4$. The $AuBr_3$ appeared reasonably stable, but due to its black color, a visual observation of any decomposition was difficult. We attempted to prepared AuI_3, but it appears that this unstable compound decomposed into AuI and elemental iodine before the experiment could be completed. The isomer shift and quadrupole splitting results of AuI and "AuI_3" are equal within experimental error. The Mössbauer spectrum of "AuI_3" is given in Fig. 4, next to that of AuI, for visual comparison "AuI_3" has a broadened linewidth which may indicate that there was some residual AuI_3 which had not undergone decomposition.

The coordination of gold in these compounds is essentially square-planar. The known bond length and bond angle information[25] for $AuCl_3$ is depicted in Fig. 13. Bonamico et al.[26] have determined the crystal structure of $NaAuCl_4$. They found the $AuCl_4^-$ ion to be essentially square-

planar, with all four Cl-Au-Cl angles being within 1° of 90°, and an average Au-Cl bond distance of 2.28 Å.

In Table III the present results for auric chlorides and bromides are compared with earlier work from this Laboratory.[2] The agreement is satisfactory in view of the lower accuracy of the earlier work and the fact that it did not reveal the quadrupole interaction.

F. $KAu(CN)_2X_2$, X = Cl, Br, I

The trans-dicyanodihaloaurate(III) complexes gave well-resolved doublets, as shown in Fig. 14. Figure 15 illustrates the trans-symmetry of the cyanide and halide ligands, which form a square-planar configuration around the gold atom.[28] The line intensities of the two quadrupole components are approximately equal; however, the lower-velocity line is in each case slightly more intense. This may be due to the Gol'danskii effect[27] or to a crystallographically non-isotropic sample. These compounds formed needle-like crystals. It is possible that these needle crystals may not have been thoroughly crushed, resulting in a partial alignment of the needle crystals in the plane of the absorber disc.

G. $KAu(CN)_4$

This substance has the largest observed quadrupole splitting and the most positive isomer shift of the auric compounds. The lines are (Fig. 16) well-resolved and, as in the three $KAu(CN)_2X_2$(X = Cl, Br, I)

compounds, the line intensities are almost, but not exactly equal. The symmetry around gold is a slightly distorted square-planar configuration. However, the linewidths and intensities were constrained to be equal in our fitting of the data.

H. Au_2O_3, $[(C_2H_5)_4N]^+[AuS_4C_4(CN)_4]^-$ and $Cs_2Au(I)Au(III)Cl_6$

The Mössbauer spectra of Au_3O_3, $[(C_2H_5)_4N]^+[AuS_4C_4(CN)_4]$ and $Cs_2Au(I)Au(III)Cl_6$ are grouped together in Fig. 17 because either the crystal structure or the purity of the compounds or both are in some question.

The crystal structure of Au_2O_3, a brown powder, has not been determined. Lacking structural information, we have simply assumed that Au_2O_3 has square-planar (axial) symmetry as do other known gold(III) compounds, and fitted the spectrum with two lines of equal linewidths and intensities.

The structure of $[AuS_4C_4(CN)_4]^-$ has not been determined crystallographically, but it has been deduced to be square-planar at gold:[29]

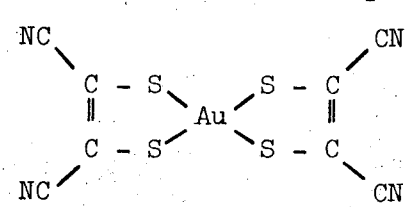

The Mössbauer spectrum of $[AuS_4C_4(CN)_4]^-$ is asymmetric, as seen in Fig. 17. The possible causes of this asymmetry are: chemically inequivalent gold atoms, partially oriented crystallites, or the Gol'danskii effect. The first possibility would probably result in more than the two (doublet) lines of square-planar $[AuS_4C_4(CN)_4]^-$. Fitting the spectrum with a single

line in addition to a doublet gave a single line at 0.121(11) cm/sec and a doublet, split by 0.197(6) cm/sec, centered about 0.326(7) cm/sec. The remaining three possibilities would (probably) involve two lines of unequal intensities. Since $[(C_2H_5)_4N]^+[AuS_4C_4(CN)_4]^-$ forms needlelike crystals, a partial orientation of incompletely crushed crystals in the plane of the absorber disc is a distinct possibility. Fitting the spectrum with two lines of equal linewidths but unequal intensities gave lines at 0.364 and 0.146 cm/sec.

The Mössbauer spectrum obtained for $Cs_2Au(I)Au(III)Cl_6$ shows a wide, unresolved absorption area. This black compound consists of equal parts gold(I) and gold(III) oxidation states.[30] It is diamagnetic,[31] so gold is not in the divalent state. The structure is known to have tetragonal symmetry, containing complex ions of linear $[AuCl_2]^-$ and square-planar $[AuCl_4]^-$ units.[32] Since $Cs_2Au(I)Au(III)Cl_6$ contains both the aurous and auric chlorides, the observed parameters for AuCl and $KAuCl_4$ were used as a first approximation to fit the $Cs_2Au(I)Au(III)Cl_6$ Mössbauer spectrum. The results are consistent with this interpretation (see Table IV below).

I. Gold Sulfides: Au_2S, Au_2S_2 and Au_2S_3

The three gold sulfide compounds were reasonably stable and sparingly soluble in water. Our samples appeared amorphous in x-ray studies.

Crystalline Au_2S was studied by some French investigators[33] who determined that Au_2S belongs to the O_h^4 Pn3m space group of Cu_2O type structure and has cubic symmetry. The Au_2S Mössbauer spectrum was fitted with two Lorentz lines of unequal intensities but of equal linewidths as shown in Fig. 18. The linewidth and two line positions are 0.249(4) cm/sec, 0.433(7) cm/sec, and -0.156(6) cm/sec, respectively.

Au_2S_2, which is diamagnetic, was not completely amorphous to x-ray powder studies, having lines similar to those of gold metal. The Mössbauer spectrum for Au_2S_2 is also shown in Fig. 18. The spectrum was fitted with four Lorentzians, with no knowledge of the Hamiltonian. This compound may be a combination of gold in both the univalent and trivalent oxidation states and may even contain some metallic gold. The linewidths were constrained to be equal and the four lines were fitted at -0.344(11) cm/sec, -0.197(15) cm/sec +0.021(58) cm/sec and +0.290(11) cm/sec. The linewidth determined by the fit was 0.326(8).

Au_2S_3 is a black powder which decomposes into its elements at about 200° C. The Mössbauer spectrum for Au_2S_3 is a complicated curve which we attempted to fit with three lines of equal linewidth as shown in Fig. 18. The line positions are -0.197(9), 0.050(11) cm/sec and +0.348(7) cm/sec. The linewidth determined by the fit was 0.303(16) cm/sec.

The sulfide spectra are too complex to interpret unambiguously; we shall therefore not attempt to include them in the general discussion below. The derived parameters for the other twenty compounds are set out in Table IV.

IV. COMPARISON OF RESULTS

A really definitive quantitative interpretation of our spectra would require calculations of Hartree-Fock quality for the gold complexes studied. This is not feasible yet, so we shall make do with a rather crude molecular-orbital interpretation. In this section we discuss qualitative relations of the derived parameters and in Sec. V we make a tentative attempt at a quantitative treatment, using atomic functions.

First we can convert the isomer shift, IS, and the quadrupole splitting, QS, into the atomic parameters $\Delta\psi_r^2(0)$ and $q_{zz}(1 + \frac{\eta^2}{3})^{1/2}$ by using the relations

$$IS = \frac{4\pi Z e^2 R^2 c}{5E_\gamma} \left(\frac{\delta R}{R}\right) (\Delta\psi_r^2(0)) \tag{2a}$$

$$QS = \frac{1}{2}\, eQ\, q_{zz}(1 + \frac{\eta^2}{3})^{1/2} \quad . \tag{2b}$$

Most of the parameters in Eq(2a) have their usual meaning,[34] but the last two factors require comment. The differential electron density of the nucleus has a subscript r to denote that it is the relativistic value. Often one uses the nonrelativistic form $\psi^2(0)$ and corrects with a relativity factor[34] $S'(Z)$. Thus $\Delta\psi_r^2(0) = S'(Z)\, \Delta\psi^2(0)$. The nucleus factor $\delta R/R$ has been given as $+3 \times 10^{-4}$ for ^{197}Au, although we note that its magnitude is not very well known.[34] The positive sign for this parameter has received support from Patterson et al.,[35] and seems quite well established. After substitution, Eq. (2a) becomes

$$IS = 1.62 \times 10^{-27}\, \Delta\psi_r^2(0) \quad . \tag{3}$$

The asymmetry parameter η is included in Eq. (2b) because we did not determine its value experimentally and cannot rigorously derive q_{zz} from QS. For the linear aurous and square-planar auric complex ions we shall take η as zero (this would be exact for a complex ion in free space: it should be a good approximation in a lattice). Substituting the value[36] $Q = +0.594(10) \times 10^{-24} cm^2$ for the quadrupole moment of the ground state of ^{197}Au into Eq. (2b), we find

$$q(1 + \frac{\eta^2}{3})^{1/2} = 28.7 \times 10^{-15} \text{ (QS)} \quad . \tag{4}$$

Using Eq. (3) and (4), we have calculated $\Delta\psi_r^2(0)$ and $q_{zz}(1 + \frac{\eta^2}{3})^{1/2}$: the results are tabulated in Table IV.

Fitted linewidths are also given in Table IV. Although we shall not discuss these in detail, they may be compared with the natural linewidth of 0.19 cm/sec FWHM. Most of the fitted linewidths are in the range 0.20 - 0.25 cm/sec, reflecting the broadening expected using medium-thickness absorbers.

Isomer Shift Systematics

The isomer shift values of gold(I) and gold(III) compounds have been arranged in order in Fig. 19. The first observation that we can make about these results is that the range of isomer shifts is very large for both oxidation states and the two ranges almost totally overlap. Thus, it is not feasible to determine the oxidation state of gold from the isomer shift alone. From Eq. (3), a positive IS indicates that the nuclear electron density of the absorber is greater than that of the source. The shifts

observed for these compounds probably arise largely from the contribution to $\psi_r^2(0)$ of the gold 6s electrons. This 6s electron density is affected by the ligands to which the gold atoms are bonded in each compound. In Fig. 19, the more electronegative halides are near the bottom and the less electronegative cyanides are near the top of the isomer shift scale for both the gold(I) and gold(III) complexes.

From Fig. 19 we note that for a given ligand the IS value of the gold(III) compound is more positive than in the corresponding gold(I) compound. This implies that the Au atom in the gold(III) compound has a <u>greater</u> nuclear electron density than in the corresponding gold(I) compound. Compare, for example, $KAu(CN)_4$ with $KAu(CN)_2$ which have IS values of +0.421 and +0.325 cm/sec, respectively or $AuCl_3$ and AuCl with IS values of +0.057 and -0.142 cm/sec, respectively. This observation can be explained as follows.

The electron configurations of gold in the aurous and auric compounds may be approximated in a molecular-orbital picture by

$$\text{Gold(I):}\quad 5d^{10}(6s6p)^{N}$$

$$\text{Gold(III):}\quad 5d^{8}(5d6s6p^{2})^{N'} \quad .$$

To simplify this discussion, consider a hypothetical ligand, L, which forms perfectly covalent bonds with gold (N = 1, N' = 1): $[AuL_2]^-$ and $[AuL_4]^-$. Gold in $[AuL_2]^-$ would have one 6s and one 6p electron. In $[AuL_4]^-$ gold would have one 6s and two 6p electrons and a 5d hole. Although both compounds would have the same number of s electrons, the effective $\psi_r^2(0)$ for $[AuL_4]^-$ should be more than for $[AuL_2]^-$ due to lower shielding of the

6s electron in $[AuL_4]^-$ complex by the nine 5d electrons. Therefore, the IS values of the gold(III) compounds would be expected to be more positive than those of the corresponding gold(I) compounds, as observed. For $N = N' = 0$, and completely ionic bonding, the same argument applies, but shielding of the 5s electrons by the 5d's would be the major factor in this case. The $6p_{1/2}$ electrons are not expected to contribute significantly to the $\psi^2(0)$ value or to shield the 6s electrons effectively.[4]

B. Quadrupole Splitting Comparisons

The quadrupole splitting results are arranged in Fig. 20. The sign of the electric field gradient cannot be determined from these experiments, although we shall make assumptions about the signs in the discussion below. First we can make two observations from Fig. 20. The QS parameter varies in magnitude with ligand in about the same order for aurous and auric compounds, and this order is similar to that of the IS variation. Also the QS range is large for both oxidation states, with considerable overlap, so the oxidation state could not be reliably determined from QS alone.

The quadrupole Hamiltonian may be written

$$H_Q = \frac{eqQ}{4I(2I-1)} \left[3I_z^2 - I(I+1) + \eta(I_x^2 - I_y^2)\right] \quad . \qquad (5)$$

To assign a sign to the quadrupole splitting, $QS = eqQ\left(1 + \frac{\eta^2}{3}\right)^{1/2}$, we make the following arguments. Linear aurous complexes are usually regarded as having sp hybrid bonds along the symmetry axis: this would make eqQ negative. Actually any σ bonds along the axis would produce an $eqQ < 0$. The observation that QS is always fairly large in Au(I) compounds supports this interpretation.

In square-planar auric compounds the situation is more complicated. If the complexes were highly ionic the Au atom would have a d^8 configuration, with the $d_{x^2-y^2}$ orbital empty. This would correspond to a concentration of negative charge density along the symmetry axis (relative to spherical symmetry), or $eqQ < 0$. Covalent dsp^2 bonding, on the other hand, tends to produce an excess of negative charge in the plane perpendicular to the tetragonal axis. Calculations show that this contribution to eqQ can be larger in magnitude than that from the $(d_{x^2-y^2})^{-2}$ configuration. Thus in passing from a purely ionic square-planar case to a completely covalent case, i.e., from $(5d_{x^2-y^2})^{-2}$ to $(5d_{x^2-y^2})^{-1}\ 6s6p^2$, the quantity eqQ is expected to vary in sign from negative to positive. We note further that the p-electron contributions to dsp^2 and sp bonds have the same magnitude but opposite signs. Thus for a given degree of covalency per bond the Au(III) complexes should have an eqQ smaller than the corresponding Au(I) complexes, because of the cancellation in eqQ due to the d^8 configuration. That these expectations are all borne out is clear on inspection of Fig. 20.

C. The Isomer Shift-Quadrupole Splitting Correlations

From Figs. 19 and 20 and the accompanying discussion, we would expect correlations between the IS and QS parameters. The theoretical basis for this is especially plain in the Au(I) case. We can describe a trend from more ionic to more covalent complexes in terms of an increasing admixture of a covalent sp component into the total wave function. Thus the 6s population should be proportional to the 6p population, or the IS and QS should be linearly related. Figure 21 shows that this is the case for

aurous halides. The relation can be described by the least-squares fitted equation

$$IS(Au(I)) = 0.782\ (QS) - 0.474\ cm/sec \quad . \tag{6}$$

For the auric compounds an IS-QS relationship is also expected, and it should probably also be linear. The situation is more complicated for the Au III compounds because both the ionic $(d_{x^2-y^2})^{-2}$ configuration and the covalent dsp^2 configuration contribute to both IS and QS. Furthermore eqQ can have either sign. We have assumed the auric fluorides to be the most ionic and accordingly assigned to their eqQ parameters the negative sign expected if the $(d_{x^2-y^2})^{-2}$ ionic configuration dominates eqQ. With this assumption the auric complexes show a good linear correlation, as shown in Fig. 22. Using only the (assumed) truly square complexes AuF_4^-, $AuCl_4^-$, $AuBr_4^-$, and $Au(CN)_4^-$, we least-squares fitted the straight line given by

$$IS(Au(III)) = 0.542\ (QS) + 0.016\ cm/sec \quad . \tag{7}$$

Since the straight lines described by Eqs. (6) and (7) do not cross, we infer that <u>the isomer shift and quadrupole splitting taken together determine the oxidation state</u>.

The three cyanohalides lie well above the line implied by Eq. (7) (see Fig. 22). This is expected because the asymmetry in the field gradient, η, will enhance QS. Because the QS values for Au(I) cyanides and halides lie at opposite ends of the scale, large values of η^2 are expected for <u>trans</u>-cyanohalides. By comparing the observed QS for these

three compounds with those calculated from their isomer shifts and Eq. (7), we can estimate η^2. The results are given in Table V. We cannot of course take this type of estimate literally, and the η^2 values in excess of 1 are clearly wrong, but the result that η^2 does turn out to be of order unity supports our expectation that it should be large for these complexes.

V. INTERPRETATION

Lacking a self-consistent field calculation, we shall interpret the structural IS and QS parameters in terms of a very simple molecular-orbital model. Atomic wave functions will be used to estimate $\Delta\psi^2(0)$ and q. Writing a bonding orbital for a gold-ligand (Au-L) bond as

$$\psi(AuL) = \alpha\ \psi(Au) + \gamma\ \psi(L) \quad ,$$

we have

$$\alpha^2 + \gamma^2 = 1 \quad ,$$

if overlap is neglected. For linear, sp-bonded aurous complexes, the molecular orbitals may be written

$$\psi_{\pm z}(AuL_2) = \frac{\alpha}{\sqrt{2}}\left[(6s) \pm (6p_z)\right] \mp \sqrt{1-\alpha^2}\ \psi(L) \quad ,$$

while for square-planar auric complexes the four orbitals are

$$\psi_{\pm x}(AuL_4) = \frac{\beta}{2}\left[(6s) \pm \sqrt{2}(6p_x) - (5d_{x^2-y^2})\right] \mp \sqrt{1-\beta^2}\ \psi(L)$$

$$\psi_{\pm y}(AuL_4) = \frac{\beta}{2}\left[(6s) \pm \sqrt{2}(6p_y) + (5d_{x^2-y^2})\right] \mp \sqrt{1-\beta^2}\ \psi(L) \quad .$$

The electric field gradient at the gold nucleus can be evaluated as

$$q_{zz} = e\langle \psi(AuL_n)\left|\frac{3\cos^2\theta - 1}{r^3}\right|\psi(AuL_n)\rangle \quad ,$$

where $n = 2$ or 4 and θ is taken with respect to the z symmetry axis with the origin of coordinates at the gold nucleus. Because of the r^{-3} term in q only the gold atomic functions contribute appreciably to q_{zz}. Thus

$$q_{zz}(AuL_2) \cong 2\alpha^2 q(6p_z) \tag{8a}$$

$$q_{zz}(AuL_4) = 2\beta^2 [q(6p_x) + q(6p_y) + q(5d_{x^2-y^2})] \quad , \tag{8b}$$

where we have taken explicit note of the fact that these equations give only the contributions of the gold-ligand bonds to q_{zz}. Before proceeding we note that a complete treatment would include a lattice contribution, a contribution from the ionic configuration, and a shielding correction to the bond contribution:

$$q_{zz} = (1 - \gamma_\infty)q^{latt} + q^{ion} + (1-R)q^{bond} \quad . \tag{9}$$

The shielding factor R for $5d$ and $6p$ electrons is unknown, and we shall neglect it. The antishielding factor, γ_∞, is perhaps as large as -42.4,[37] the value for Bi^{3+}. Even so, we estimate that $(1-\gamma_\infty)q^{latt}$ is only 6×10^{13} esu or smaller.[38] In Au(I)($5d^{10}$) the $5d^{10}$ core is spherically symmetrical and $q^{ion} \equiv 0$. In Au(III)($5d^8$) the $5d^8$ core gives a contribution $q^{ion} \equiv -2q(5d_{x^2-y^2})$. Changing now to an angular momentum basis, and using the relations

$$q_{zz}(5d_{x^2-y^2}) = q_{zz}(522)$$

$$q_{zz}(6p_z) = q_{zz}(610) \quad ,$$

where for example (610) represents $n = 6$, $\ell = 1$, $m_\ell = 0$, we may combine Eqs. (8) and (11) to read

$$q_{zz}(AuL_2) = 2\alpha^2 q_{zz}(610) \tag{10a}$$

$$q_{zz}(AuL_4) = -2q_{zz}(522) + 2\beta^2[q_{zz}(522) + 2q_{zz}(611)] \quad . \tag{10b}$$

Thus calculation of q_{zz} requires the evaluation of the atomic parameters $q_{zz}(611)$ and $q_{zz}(522)$. Evaluating the angular factor, we can write $q_{n\ell\ell} = e(2\ell)(2\ell + 3)^{-1} \langle r^{-3} \rangle_{n\ell}$. Thus

$$q_{610} = 2q_{611} = 1.29 \times 10^{15} \langle r^{-3} \rangle_{61} \tag{11a}$$

$$q_{522} = 1.84 \times 10^{15} \langle r^{-3} \rangle_{52} \quad , \tag{11b}$$

if $\langle r^{-3} \rangle$ is given in units of a_o^{-3} and q in units of esu/cm^3.

For the 5d core the evaluation of $\langle r^{-3} \rangle$ was not difficult. Although there is some ambiguity about just which ionic configuration of the free ion should be used in calculating $\langle r^{-3} \rangle_{5d}$, the choice isn't critical because this parameter is not very sensitive to the configuration chosen. Of more concern is the difference between $\langle r^{-3} \rangle_{5d}$ for the $5d_{3/2}$ and $5d_{5/2}$ shells, which are considerably different in a heavy atom like gold, where relativistic effects are important. We used the results of Dirac-Fock calculations for several configurations kindly provided by

J. B. Mann.[39] After a somewhat complicated fitting procedure[38] we adopted the value

$$\langle r^{-3} \rangle_{5d} = 14.5\ a_o^{-3}$$

or

$$q_{522} = 26.9\ \text{esu cm}^{-3} \quad ,$$

as being appropriate for neutral gold in the $5d^8(dsp^2)^n$ configuration (i.e., for $n = 3/4$). This value is in fair agreement with the values of $12.3\ a_o^{-3}$ and $11.8\ a_o^{-3}$ obtained from magnetic hfs and atomic fine structure results.[40]

We found $\langle r^{-3} \rangle_{6p}$ much more difficult to estimate. The range of experimental quadrupole splittings (QS) requires, on our bonding model, that $\langle r^{-3} \rangle_{6p}$ be quite large, probably substantially in excess of the value $8.9\ a_o^{-3}$ found[41,42] for Hg in $HgCl_2$. One would expect a priori that the values of $\langle r^{-3} \rangle_{6p}$ for Au and Hg would be about the same.

Our attempts to estimate an appropriate $\langle r^{-3} \rangle_{6p}$ from the results of free-atom calculations were not successful. A direct calculation on Au $(5d^{10}6s6p)$ is not feasible, and even in the Au $(5d^{10}6p)$ state the 6p electron is too weakly bound to give a realistic result. We therefore tried various extrapolation schemes (a total of five) using atomic Hartree-Fock and Dirac-Fock results on neighboring atoms or ions in which the 6p electron was more tightly bound.[43] The results were very disappointing. The extrapolated values for $\langle r^{-3} \rangle_{6p}$ in neutral gold were very low ($\leq 5\ a_o^{-3}$), and different extrapolation procedures gave widely varying results. We have

little doubt that the atomic $\langle r^{-3} \rangle_{5p}$ values were reliable: four different methods--Dirac-Fock,[39] Slater-Hartree-Fock,[44] and two variants of Hartree-Fock[45,46,47]--gave results that agreed quite well. We could, however, find no convincing way to extrapolate these results to the case of interest. The one positive result of these calculations is the conclusion that $\langle r^{-3} \rangle_{6p}$ for neutral gold is probably not larger than about 5 a_o^{-3}. We shall see below that <u>this value is too small to account for the observed QS in terms of 6s6p hybrid bonds</u>. This conclusion also applies to the $HgCl_2$ results of Dehmelt, <u>et al</u>.[42] We are therefore faced with a choice in interpretation at this point: (1) we can give up the sp hybrid model, or (2) we can "parameterize" q_{610}; that is, admit that it cannot be evaluated from atomic wave functions and try instead to determine it empirically. We have chosen this second alternative.

The observed isomer shift between two compounds is given by Eq. (3). If we parameterize $\delta R/R$, this becomes

$$IS = 5.4 \times 10^{-24} \left(\frac{\delta R}{R}\right) \Delta \psi_r^2(0) \quad . \tag{12}$$

Now the IS between any two aurous compounds could be calculated if α and $\delta R/R$ were known, and similarly for the auric series. The values of $\psi_r^2(0)$ for the configurations corresponding to the values $\alpha^2 = 0, 1/2$, and $\beta^2 = 0, 1/2$, taken from Mann's Dirac-Fock calculations, are set out in Table VI. Now we can relate $\delta R/R$ to q_{610} for aurous compounds, and to q_{610} and q_{522} for auric compounds, because we know the variation of IS with QS, even though we do not know α or β for any component. Evaluating Eq. (10) at $\alpha^2 = 0, 1/2$ and $\beta^2 = 0, 1/2$, and using Eqs. (5-7), and

$Q = 0.595 \times 10^{-24}$ cm^2, $\eta = 0$, we find

$$IS(AuI,\ \Delta\alpha^2 = 1/2) = -0.391\ \frac{ceQ}{E_\gamma}\ q_{610} \tag{13a}$$

$$IS(AuIII,\ \Delta\beta'^2 = 1/2) = 0.271\ \frac{ceQ}{E_\gamma}\ (q_{610} - q_{522})\ , \tag{13b}$$

where we have used $q_{610} = -2q_{611}$. Substituting for IS now from Eq. (12), using the appropriate values from Table VI, we find finally

$$\delta R/R = -7.15 \times 10^{-21}\ q_{610} \tag{14a}$$

$$\delta R/R = 4.44 \times 10^{-21}\ (q_{522} - q_{610})\ , \tag{14b}$$

where these two equations have been derived from (13a) and (13b), respectively. Here q_{610} and q_{522} are in cgs-esu and $\delta R/R$ is dimensionless. Replacing q_{522} by its numerical value of 26.9×10^{15} esu/cm^3, we have two equations and two unknowns: $\delta R/R$ and q_{610}. The solutions are

$$\delta R/R = +3.1 \times 10^{-4}$$

$$q_{610} = -44 \times 10^{15}\ \text{esu/cm}^3\ .$$

Although this value of $\delta R/R$ is in excellent agreement with the earlier estimate,[34] neither was very well-founded, and we do not believe that this agreement should be taken seriously. Probably we are pushing the simple molecular-orbital model too far in requiring Eqs. (14) to hold. The concommitant $|q_{610}| = 44 \times 10^{15}$ esn/cm^3 is much too large to be credible.

It is difficult even to reconcile the value $|q_{610}(\text{Hg in } HgCl_2)| = 23 \times 10^{15}$ esu/cm^3, which can be calculated from the results of Dehmelt et al.,[42] with values calculated from atomic functions. The extrapolated value $\langle r^{-3} \rangle_{6p} = 5a_o^{-3}$ for atomic gold corresponds to $q_{610} = -13 \times 10^{15}$ esu/cm^3.

Still if we are going to express our results in terms of sp and dsp^2 hybridization, we apparently must accept the very large $|q_{610}|$ that Eqs. (14) give us. Of course this quantity must be understood as an "effective" 6p field gradient, $q_{610}(\text{eff})$, that must be associated with some more subtle property of the linear or square-planar bonds than just the charge distribution of a single 6p electron (because $\langle r^{-3} \rangle_{6p}$ would then be too large). It would be tempting to suppose that exact satisfaction of Eqs. (14) was not really required, but that we could allow $|q_{610}(\text{eff})|$ to be as small as 25×10^{15} esu cm^{-3}, for example, rationalizing that the resultant discrepancy in $\delta R/R$ ($+1.8 \times 10^{-4}$ for Au(I) versus $+2.3 \times 10^{-4}$ for Au(III)) was acceptable in the spirit of the model. This approach would even have the support of an empirical precedent in that the $HgCl_2$ results implied a similar value for $|q_{610}(\text{eff})|$ in Hg. Unfortunately this interpretation would lead to even worse problems, because if $|q_{610}(\text{eff})|$ were as small as 25×10^{15} esu/cm^{-3}, then α and β would have to be increased considerably to fit the experimental values of QS, and the bonds would become strongly polar toward gold. This seems rather unlikely for gold-halogen (especially Au-F) bonds. This result is illustrated in Table VII, where the charges X on the gold atoms, calculated from

$$X(\text{AuI}) = 1 - 4\alpha^2$$

$$X(\mathrm{AuIII}) = 3 - 8\beta^2 \quad ,$$

have been calculated from the experimental values of QS, together with Eqs. (10) and the two values $q_{610} = -25$ and -44×10^{15} esu cm^{-3}. Since the charges on Au are unreasonably negative for the former value we are inclined to favor the latter, although it is much larger than we would calculate using atomic orbitals.

VI. SUMMARY

From the Mössbauer experiment results of the linear gold(I) and square-planar gold(III) compounds, direct relationships were established between the isomer shifts and quadrupole splittings for both oxidation states of gold. These relationships were explained in terms of the hybridization of the bonds and the number of bonding electrons on gold. The results suggest that the hybridizations of the compounds may remain essentially constant, sp for the gold(I) and dsp^2 for the gold(III) compounds, and that the changes in the isomer shift and quadrupole splittings may be due to the differences in the ionic character of the various compounds.

We attempted to determine the values of q_{522} and q_{610} from Dirac-Fock free-atom wave functions of gold which were calculated by Mann. For q_{522}, we deduced a value of 26.9×10^{15} esu/cm^3. The parameter q_{522} was not a sensitive function of charge. Unfortunately, the q_{610} value was much more difficult to determine and was found to be a very sensitive function of charge. From the free-atom wave functions, we estimated q_{610} for neutral Au to be quite small, perhaps $-(10\text{-}15) \times 10^{15}$ esu/cm^3. However, from the results of the linear relationship of the isomer shift and quadrupole splitting for gold(I) and gold(III) compounds, and the nuclear electron density calculations, we arrived at a q_{610} value of -44×10^{15} esu/cm^3. This corresponds to a nuclear factor, $\delta R/R$, of $+3.1 \times 10^{-4}$. The charges on gold in the compounds were given for q_{610} values of -25×10^{15} and -44×10^{15} esu/cm^3. For $q_{610} = -25 \times 10^{15}$ esu/cm^3, $\delta R/R$ is about $+2 \times 10^{-4}$. Thus we can probably conclude that the nuclear factor probably lies in the range $\delta R/R = +(2.5 \pm 0.6) \times 10^{-4}$.

It appears that the free-atom wave functions are not adequate for estimating the electric field gradient for loosely bound electrons such as the 6p electrons of gold. Further insight into the bonding characteristics of these gold compounds must await molecular structure calculations which are not yet available for heavy atoms.

FOOTNOTES AND REFERENCES

* Work performed under the auspices of the U. S. Atomic Energy Commission.

1. L. D. Roberts, H. Pomerance, J. O. Thompson, and C. F. Dam, Bull. Am. Phys. Soc. 7, 565 (1962).
2. D. A. Shirley, R. W. Grant, and D. A. Keller, Rev. Mod. Phys. 36, 352 (1964).
3. C. M. Lederer, J. M. Hollander and I. Perlman, Table of Isotopes, Sixth Edition, (Wiley, 1967).
4. M. O. Faltens, Ph.D. Thesis, University of California, Lawrence Radiation Laboratory Report UCRL-18706, (1969).
5. A. G. Sharpe, Chem. Soc. (London) pt. 4, 2901 (1949).
6. H. L. Wells, Am. J. Sci. 3, 315 (1922).
7. J. C. Bailar, Jr., Inorganic Synthesis (McGraw-Hill) Vol. IV, p. 14.
8. A. B. Prescott and O. C. Johnson, Quantitative Chemical Analysis, p. 234 (Van Nostrand, 1933).
9. J. M. Smith, L. H. Jones, I. Kressen, and R. A. Penneman, Inorg. Chem. 4, 369 (1965).
10. H. Brown, J. Am. Chem. Soc. 49, 958 (1927).
11. R. Zane, University of California Lawrence Radiation Laboratory Report UCRL-16401 (1965).
12. H. H. Wickman, M. P. Klein, and D. A. Shirley, Phys. Rev. 152, 345 (1966).
13. R. S. Preston, S. S. Hanna, and J. Heberle, Phys. Rev. 128, 2207 (1962).
14. W. C. Davidon, Argonne National Laboratory Report ANL-5990 Rev. (1959).
15. H. Jagodzinski, Z. für Krist. 112, 80 (1959).
16. P. Machmer, M. Read, and P. Cornil, Compt. Rend., Ser. A, B 262B (9), 650 (1966).

17. P. Machmer Z. Naturforsch 21 (11), 1025 (1966).

18. D. H. Templeton, and H. Rubin, Department of Chemistry, University of California, Berkeley, private communication, 1968.

19. G. S. Zhdanov and E. A. Sugam, Acta. Physicochim URSS 20, 253 (1945).

20. L. H. Jones, J. Chem. Phys. 27, 468 (1957).

21. F. A. Cotton and G. Wilkinson, Advanced Inorganic Chemistry (Interscience, 1962), p. 867.

22. R. A. Penneman and E. Staristzky, J. Inorg. Nucl. Chem. 17, 45 (1958).

23. A. Rosenzweig and D. T. Cromer, Acta. Cryst. 12, 709 (1959).

24. W. B. Einstein, P. R. Rao, James Trotter, and Neil Bartlett, J. Chem. Soc., 478 (1967).

25. E. S. Clark and D. H. Templeton, Acta. Cryst. 11, 284 (1958).

26. M. Bonamico, G. Dessy, and A. Vaciago, Atti Accad. Nazl. Lincei. Rend., Classe Sci. Fis. Mat. Nat. 39 (6), 504 (1965).

27. V. I. Goldanskii, The Mössbauer Effect and its Application to Chemistry, (D. Van Nostrand Co., Inc., New York, 1966).

28. J. M. Smith, L. H. Jones, I. K. Kressin, and R. A. Penneman, Inorg. Chem. 4, 369 (1965).

29. A. Davison, N. Edelstein, R. H. Holm, and A. H. Maki, Inorg. Chem. 2, 1227 (1963).

30. H. L. Wells, Am. J. Sci. 3, 315 (1922).

31. N. Elliott, J. Chem. Phys. 2, 419 (1934).

32. N. Elliott and L. Pauling, J. Am. Chem. Soc. 60, 1846 (1938).

33. H. Hirsch, A. de Cugnac, M. C. Gadet, and J. Pouradier, Compt. Rendu. Acad. Sci. Paris, Ser. A, B 263B (23), 1328 (1966).

34. D. A. Shirley, Rev. Mod. Phys. 36, 339 (1964).

35. D. O. Patterson, L. D. Roberts, J. O. Thomson, and R. P. Levey, Oak Ridge National Laboratory Report ORNL-TM-1685 (1967).

36. A. G. Blachman, D. A. Landman, and A. Lurio, Phys. Rev. 161, 60 (1967).

37. R. M. Sternheimer, Phys. Rev. 159, 266 (1967).

38. See Ref. 4 for details of this calculation.

39. J. B. Mann, Los Alamos Scientific Laboratory (private communication, 1968).

40. W. J. Childs and L. S. Goodman, Phys. Rev. 141, 176 (1966).

41. We have calculated this value from data given in Ref. 42.

42. H. G. Dehmelt, H. G. Robinson, and W. Gordy, Phys. Rev. 93, 480 (1954).

43. See Ref. 4, pp. 143-150 for details.

44. F. Herman and S. Skillman, Atomic Structure Calculations (Prentice-Hall, New Jersey, 1963).

45. J. B. Mann, Atomic Structure Calculations II. Hartree-Fock Wavefunctions and Radial Expectation Values: Hydrogen to Lawrencium, Los Alamos Scientific Laboratory Report, LA-3691, (1968).

46. We also made Hartree-Fock calculations using C. C. J. Roothaan's programs, (see Ref. 47).

47. C. C. J. Roothaan, Rev. Mod. Phys. 23, 69 (1951); 32, 179 (1960).

Table I. Parameters for Aurous Halides.

AuCl	T° K	Isomer Shift (cm/sec)[a]	Quadrupole splitting (cm/sec)[a]
This work	4.2	-0.142 (1)	0.465 (1)
Ref. 2	4.2	-0.161 (20)	0.434 (40)
Ref. 17	300	---	triplet
			514.15 MHz = 0.4120 cm/sec
			514.346MHz = 0.4122 cm/sec
			514.754MHz = 0.4125 cm/sec
AuBr			
This work	4.2	-0.147 (1)	0.423 (4)
Ref. 2	4.2	-0.143 (10)	0.410 (20)
AuI			
This work	4.2	-0.132 (3)	0.398 (1)
Ref. 2	4.2	-0.124 (10)	0.383 (20)
Ref. 16	300	---	508.296 MHz = 0.4074
Ref. 16	77	---	triplet
			512.554 MHz = 0.4108 cm/sec
			516.554 MHz = 0.4139 cm/sec
			516.620 MHz = 0.4141 cm/sec

[a]Errors in last place indicated parenthetically.

Table II. Results for Auric Fluorides.

Compound	Isomer Shift ($\frac{cm}{sec}$)	Quadrupole Splitting ($\frac{cm}{sec}$)	Reference
AuF_3	-0.13 (2)	---	1
AuF_3	-0.107(1)	0.274(2)	This work
$KAuF_4$	0.00 (2)	---	1
$[BrF_2]^+[AuF_4]^-$	-0.069(2)	0.182(2)	This work

Table III. Auric Bromide and Chloride Parameters.

Compound	Isomer Shift ($\frac{cm}{sec}$)	Quadrupole Splitting ($\frac{cm}{sec}$)	Reference
$AuCl_3$	0.057(9)	0.075(8)	This work
	0.037(15)	---	2
$NaAuCl_4$,$KAuCl_4$	0.044(6)	0.127(8)	This work
	0.036(20)	---	2
$KAuBr_4$	0.067(2)	0.113(2)	This work
	0.015(15)	---	2

Table IV. Results of the Mössbauer Experiments

Compound	Gold Areal Density mg/cm^2	Parameters from Fits of Spectra: Isomer Shift (cm/sec) Relative to ^{197}AuPt		Quadrupole Splitting (cm/sec)	Linewidth (FWHM) cm/sec	Derived Parameters: $\Delta\psi(0)^2 \times 10^{25}$ (cm^{-3}) Relativistic	$\lvert q_{zz}(1+\frac{\eta^2}{3})^{1/2}\rvert$, units of 10^{15}esu
AuF_3	164	-0.107(1)		0.274(2)	0.232(2)	-6.61	(-) 7.86
$[BrF_2]^+[AuF_4]^-$	160	-0.069(2)		0.182(2)	0.228(40)	-4.26	(-) 5.22
AuCl	170	-0.142(1)		0.465(1)	0.196(4)	-8.77	(-)13.33
$KAuCl_4$	224	0.044(6)		0.127(8)	0.254(29)	2.71	3.64
$AuCl_3$	228	2.057(9)		0.075(8)	0.241(20)	3.52	2.15
AuBr	204	-0.147(1)		0.423(4)	0.217(8)	-9.08	(-)12.13
$KAuBr_4$	156	0.067(2)		0.113(2)	0.220(12)	4.11	3.24
$AuBr_3$	187	0.079(∿7)		0.127(∿2)	0.300(4)	4.88	3.64
AuI	527	-0.132(3)		0.398(1)	0.242(4)	-8.15	(-)11.41
"AuI_3"	583	-0.153(37)		0.399(5)	0.237(41)	-9.45	(-)11.44
$Cs_2Au_2Cl_6$		-0.143(28)	I	0.410(5)	0.216(4)		
		-0.009(22)	III	0.133(18)	0.164(6)		
AuCN	289	0.166(17)		0.809(3)	0.272(23)	10.25	(-)23.20
$KAu(CN)_2$	168	0.325(8)		1.021(6)	0.195(18)	20.08	(-)29.28
$KAu(CN)_4$	168	0.421(12)		0.699(5)	0.218(14)	26.01	20.05
$KAu(CN)_2Cl_2$	328	0.256(2)		0.526(2)	0.218(4)	15.81	∿ 12.69
$KAu(CN)_2Br_2$	119	0.272(7)		0.546(1)	0.245(25)	16.80	∿ 13.53
$KAu(CN)_2I_2$	97	0.278(6)		0.587(3)	0.215(12)	17.17	∿ 13.85
$[(C_2H_5)_4N]^+[AuS_4C_4(CN)_4]^-$		0.326(7)		0.197(6)	0.221(5)	20.14	
Au_2O_3	232	0.094(1)		0.168(4)	0.350(22)	5.80	4.81
$Na_3Au(S_2O_3)_2$		0.072(29)		0.708(4)	0.317(20)	4.44	(-)20.31

Table V. Estimates of η^2 for the potassium dicyanodihaloaurates.

Compound	IS (cm/sec)	QS(calc) for η=0 (cm/sec)	QS observed cm/sec	η^2 calculated
$KAu(CN)_2Cl_2$	0.256	0.442	0.526	1.114
$KAu(CN)_2Br_2$	0.272	0.471	0.546	1.007
$KAu(CN)_2I_2$	0.278	0.482	0.587	1.196

Table VI. Values of $\Delta\psi^2(0)$ for gold(I) and gold(III) states for which α^2, $\beta^2 = 0$ and 1/2.

α^2	State Required	State Calculated	Units of $\Sigma\psi^2(0)$, 10^{26} cm^{-3}
	Au(I)		
0	$5d^{10}$	$5d^{10}$	$\sum_{n=1}^{5} \psi^2(0)_{ns}$ = 129099.743
1/2	$5d^{10}6s6p$	$5d^{10}6s$	$\sum_{n=1}^{6} \psi^2(0)_{ns}$ = 129106.825
			$\Delta\psi^2(0)_{ns}$ = -7.08_2
			Au(I)
β^2	Au(III)		
0	$5d^8$	$5d^8 6s$	$\sum_{n=1}^{5} \psi^2(0)_{ns}$ = 129102.601
1/2	$5d^9 6s6p^2$	$5d^9 6s$	$\sum_{n=1}^{6} \psi^2(0)_{ns}$ = 129110.182*
		$5d^9 6p$	$\psi^2(0)_{6p^2}$ = 0.327**
			$\Delta\psi(0)^2$ = -7.908
			Au(III)

*,** The difference in shielding of $\sum_{n=1}^{5} \psi^2(0)_{ns}$ by the 6s and 6p electrons is only about 5 parts in 10^6. Therefore we approximated $\psi(0)^2_{total}$ of $\beta = 1/2$ by summing the two $\psi^2(0)$ values.

Table VII. Charges on gold atoms in various compounds.

Compound	q_{zz} (a)	$q_{610} = -25$		$q_{610} = -44$	
		α^2 or β^2	X	α^2 or β^2	X
Gold(I)					
AuCl	13.3	0.27	-0.07	0.15	0.41
AuBr	12.1	0.24	0.03	0.14	0.46
AuI	11.4	0.23	0.09	0.13	0.49
$Na_3Au(S_2O_3)_2$	20.3	0.41	-0.62	0.23	0.10
AuCN	23.2	0.46	-0.86	0.26	-0.03
$KAu(CN)_2$	29.3	0.59	-1.34	0.33	-0.30
Gold(III)					
AuF_3	-7.9	0.44	-0.54	0.32	0.41
$[BrF_2]^+[AuF_4]^-$	-5.2	0.47	-0.74	0.34	0.26
$KAuCl_4$	3.6	0.55	-1.42	0.40	-0.24
$AuCl_3$	2.2	0.54	-1.31	0.39	-0.15
$KAuBr_4$	3.2	0.55	-1.39	0.40	-0.21
$AuBr_3$	3.6	0.55	-1.42	0.40	-0.24
$KAu(CN)_4$	20.1	0.71	-2.69	0.52	-1.16
$KAu(CN)_2Cl_2$	∿12.7	0.64	-2.12	0.47	-0.75
$KAu(CN)_2Br_2$	∿13.5	0.65	-2.19	0.47	-0.80
$KAu(CN)_2I_2$	∿13.9	0.65	-2.21	0.48	-0.81
$[(C_2H_5)_4N]^+$ $[AuS_4C_4(CN)_4]^-$	5.7	0.57	-1.58	0.42	-0.35
Au_2O_3	4.8	0.56	-1.52	0.41	-0.30

(a) q_{zz}, q_{610} are in units of 10^{15} esu/cm^3.

FIGURE CAPTIONS

Fig. 1. Decay scheme of ^{197}Pt after Ref. 3.

Fig. 2. Flow sheet showing preparation of gold compounds.

Fig. 3. Schematic diagram of the Mössbauer spectrometer circuit.

Fig. 4. Spectra of aurous halides, with fitted Lorentzian curves.

Fig. 5. Coordination of Au in AuI, after Ref. 15.

Fig. 6. Mössbauer spectrum of sodium dithiosulfatoaurate dihydrate.

Fig. 7. Coordination of gold in sodium dithiosulfatoaurate dihydrate, after Templeton and Rubin, Ref. 18.

Fig. 8. Spectra of the Gold cyanides.

Fig. 9. Coordination of gold in $KAu(CN)_2$, after Ref. 23.

Fig. 10. Spectra of Auric fluorides.

Fig. 11. Gold coordination in AuF_3, after Ref. 24.

Fig. 12. Auric bromide and chloride spectra.

Fig. 13. Structure of $(AuCl_3)_2$ dimer, after Ref. 25.

Fig. 14. Spectra of potassium trans-dicyanodihaloaurates.

Fig. 15. Coordination of gold in the trans-dicyanodihaloaurate complexes, as given in Ref. 28.

Fig. 16. Spectrum of $KAu(CN)_4$.

Fig. 17. Mössbauer spectra of three gold compounds. The salt $[(C_2H_5)_4N]^+[AuS_4C_4(CN)_4]^-$ was used for the middle spectrum.

Fig. 18. Spectra of gold sulfides.

Fig. 19. Comparison of isomer shifts.

Fig. 20. Comparison of quadrupole splittings.

Fig. 21. Linear relation of QS and IS for aurous compounds.

Fig. 22. Linear relation of QS and IS for auric compounds.

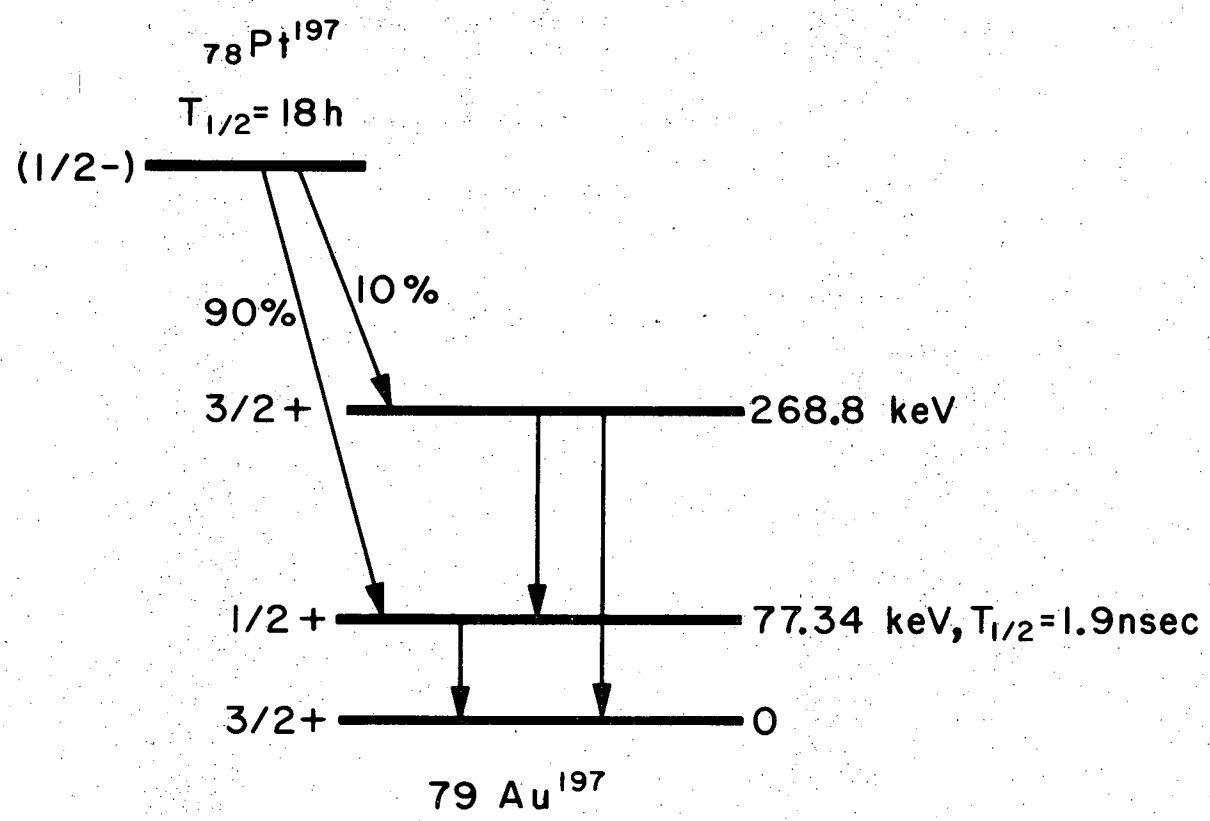

XBL702-2364

Fig. 1

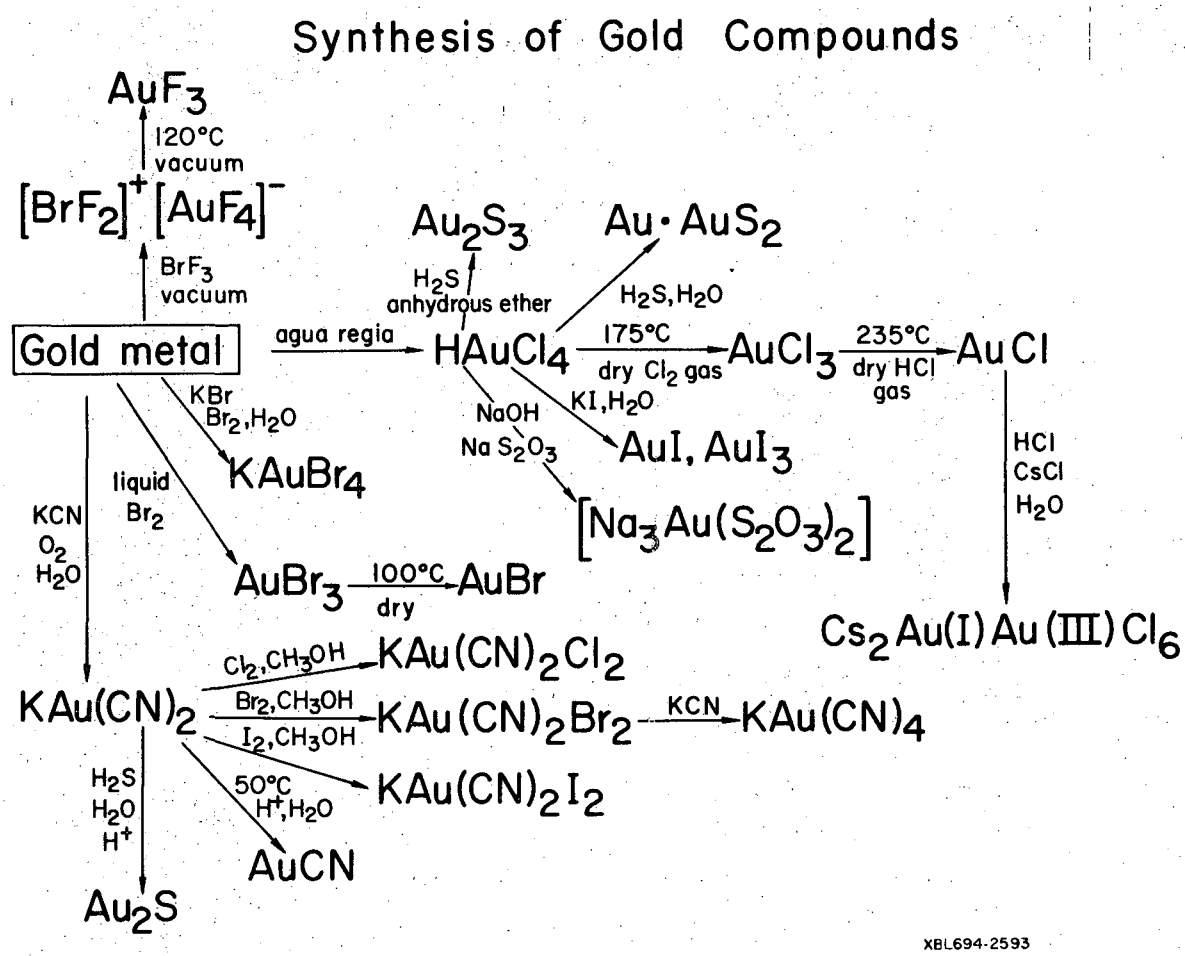
Synthesis of Gold Compounds
AuF3
120°C
vacuum
[BrF2]+ [AuF4]−
BrF3
vacuum
Gold metal
agua regia
HAuCl4
H2S
anhydrous ether
Au2S3
Au · AuS2
H2S, H2O
175°C
dry Cl2 gas
AuCl3
235°C
dry HCl
gas
AuCl
KI, H2O
AuI, AuI3
NaOH
Na S2O3
[Na3Au(S2O3)2]
KBr
Br2, H2O
KAuBr4
liquid
Br2
AuBr3
100°C
dry
AuBr
KCN
O2
H2O
HCl
CsCl
H2O
Cs2Au(I)Au(III)Cl6
KAu(CN)2
Cl2, CH3OH
KAu(CN)2Cl2
Br2, CH3OH
I2, CH3OH
KAu(CN)2Br2
KCN
KAu(CN)4
KAu(CN)2I2
50°C
H+, H2O
AuCN
H2S
H2O
H+
Au2S
XBL694-2593

Fig. 2.

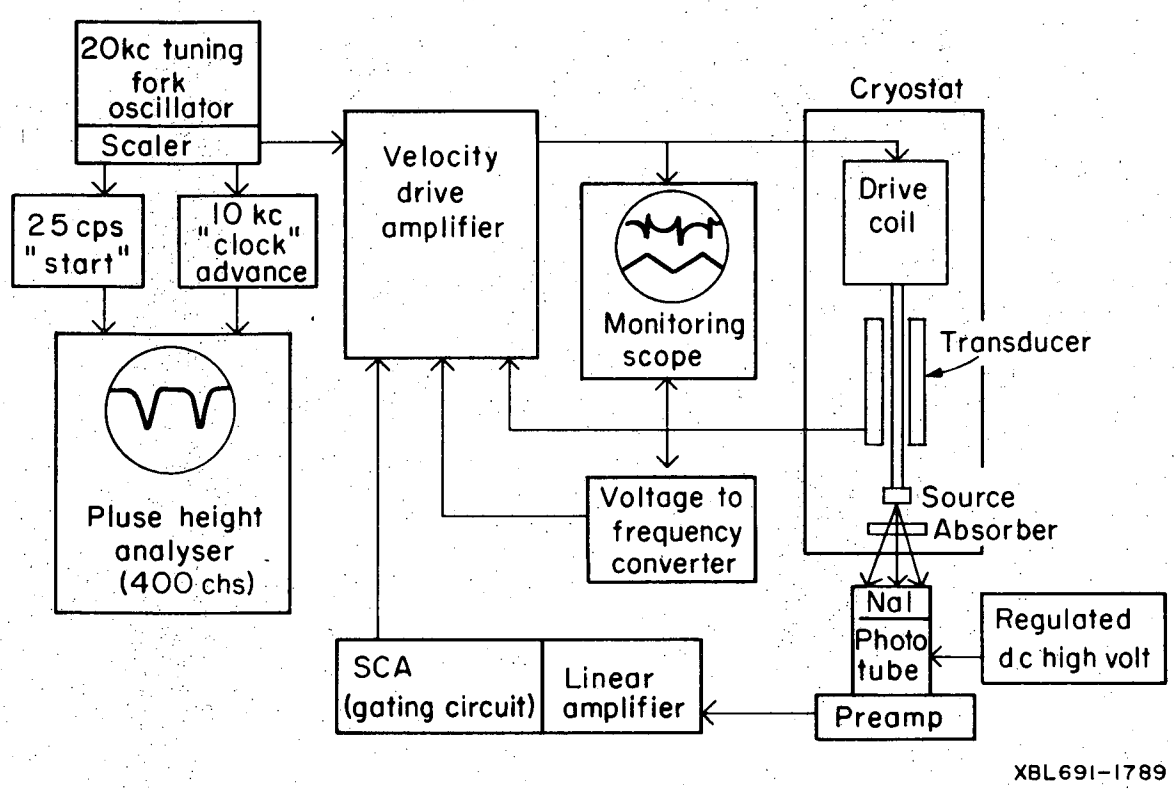
20kc tuning fork oscillator
Scaler
25 cps "start"
10 kc "clock" advance
Pluse height analyser (400 chs)
Velocity drive amplifier
Monitoring scope
Voltage to frequency converter
Cryostat
Drive coil
Transducer
Source
Absorber
NaI
Photo tube
Regulated dc high volt
Preamp
Linear amplifier
SCA (gating circuit)
XBL691-1789

Fig. 3.

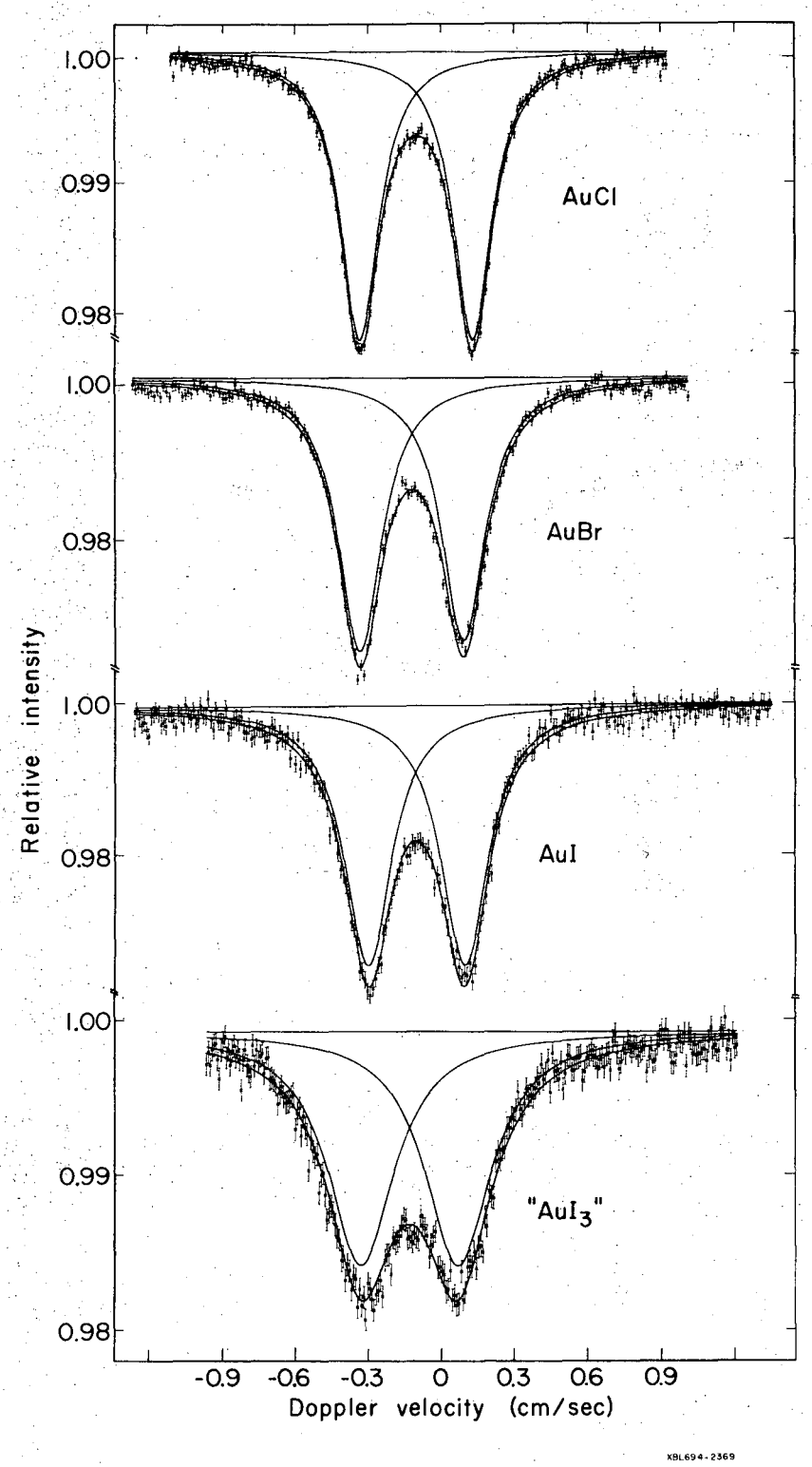
1.00
0.99
0.98
AuCl
1.00
0.98
AuBr
1.00
0.98
AuI
1.00
0.99
0.98
"AuI3"
Relative intensity
-0.9 -0.6 -0.3 0 0.3 0.6 0.9
Doppler velocity (cm/sec)
XBL694-2369

Fig. 4.

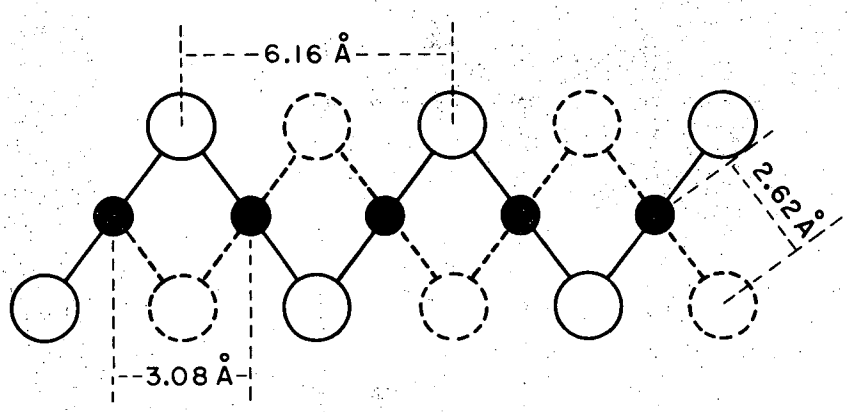

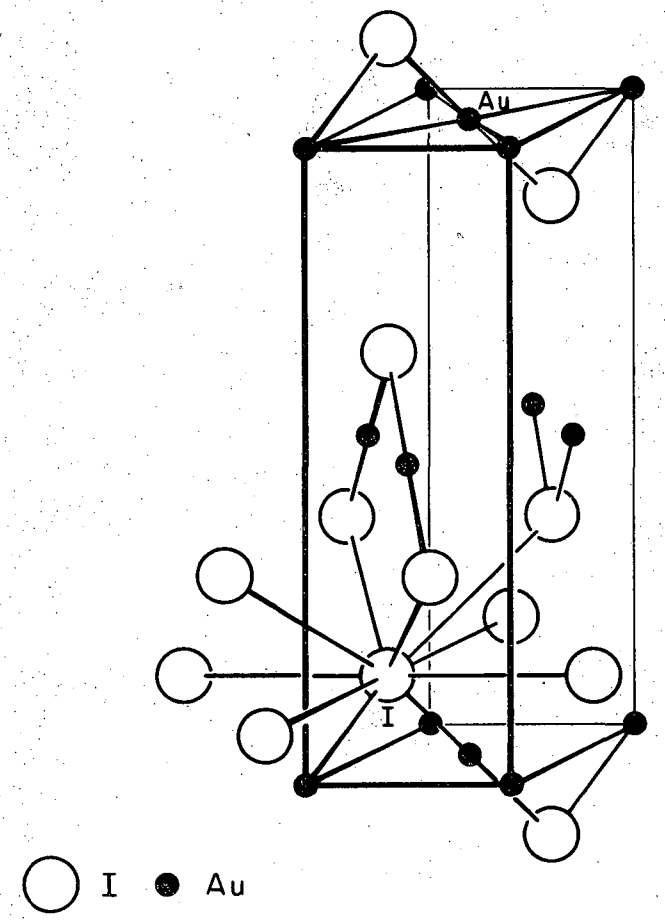

XBL691-1782

Fig. 5.

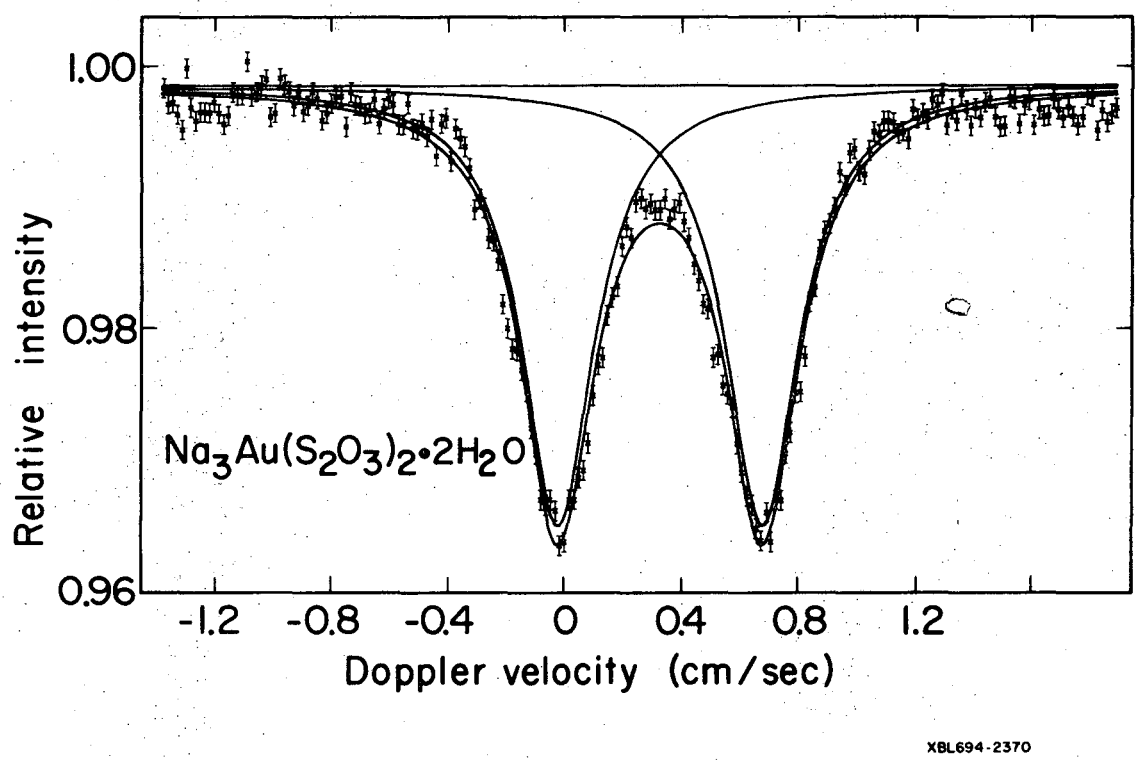
1.00
0.98
0.96
Relative intensity
$Na_3Au(S_2O_3)_2 \cdot 2H_2O$
-1.2
-0.8
-0.4
0
0.4
0.8
1.2
Doppler velocity (cm/sec)
XBL694-2370

Fig. 6.

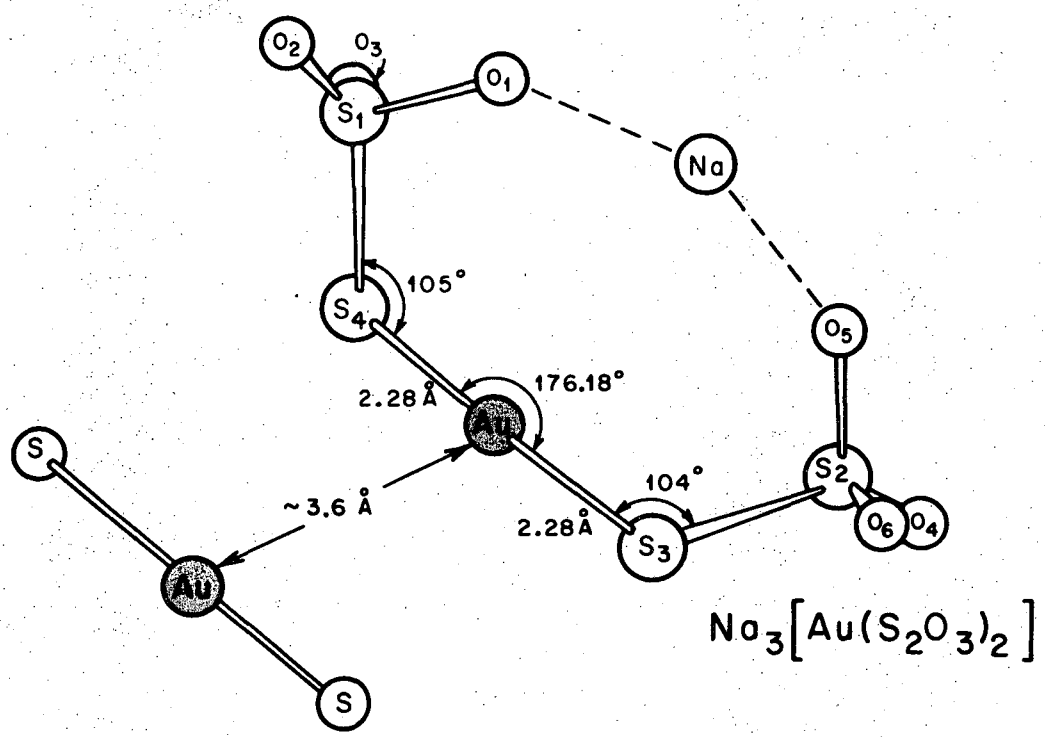
O2
O3
O1
S1
Na
105°
S4
O5
2.28 Å
176.18°
Au
S
~3.6 Å
104°
S2
2.28 Å
S3
O6
O4
Au
S
Na3[Au(S2O3)2]

Fig. 7

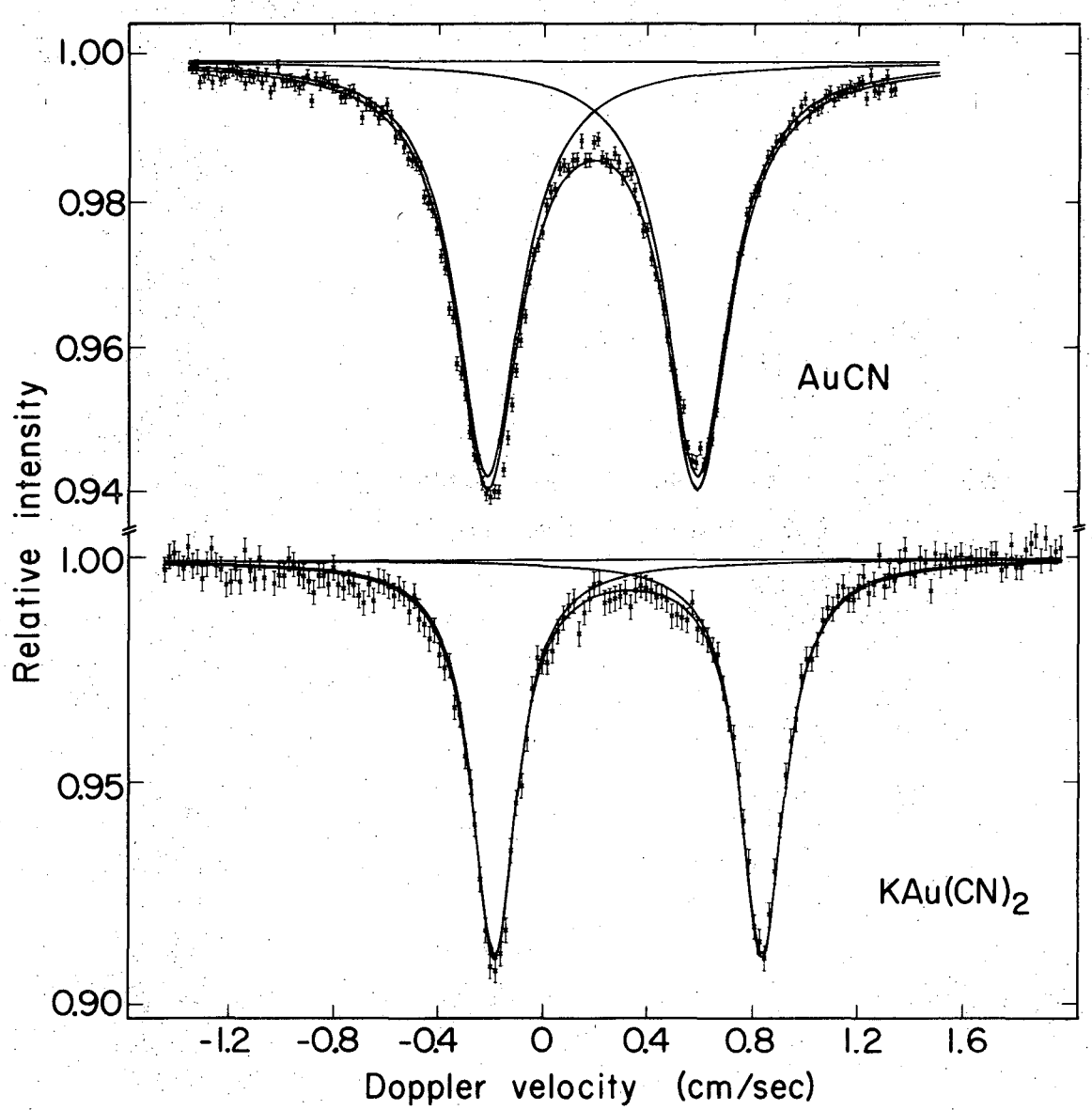

XBL694-2371

Fig. 8.

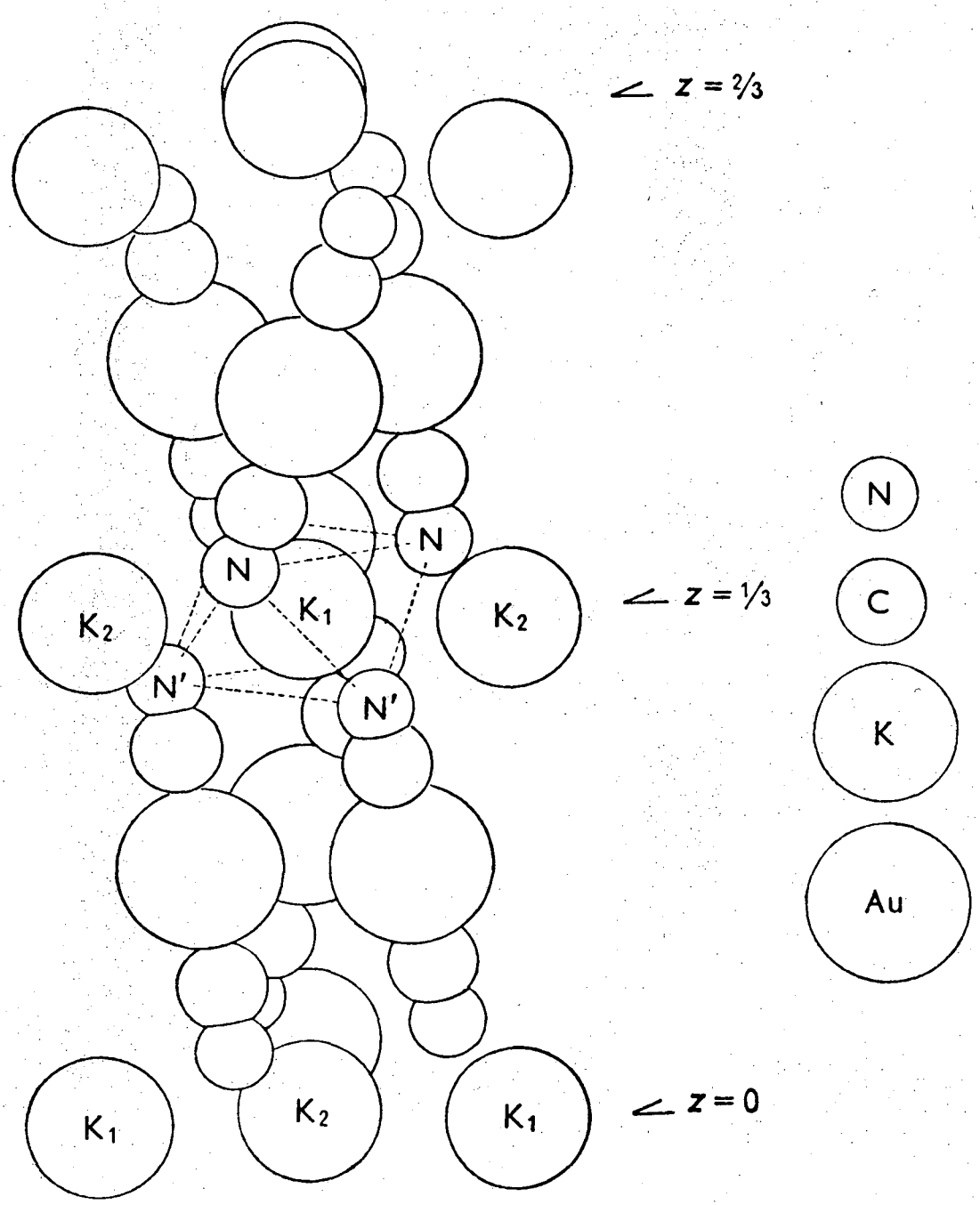

XBL 6811-6161

Fig. 9.

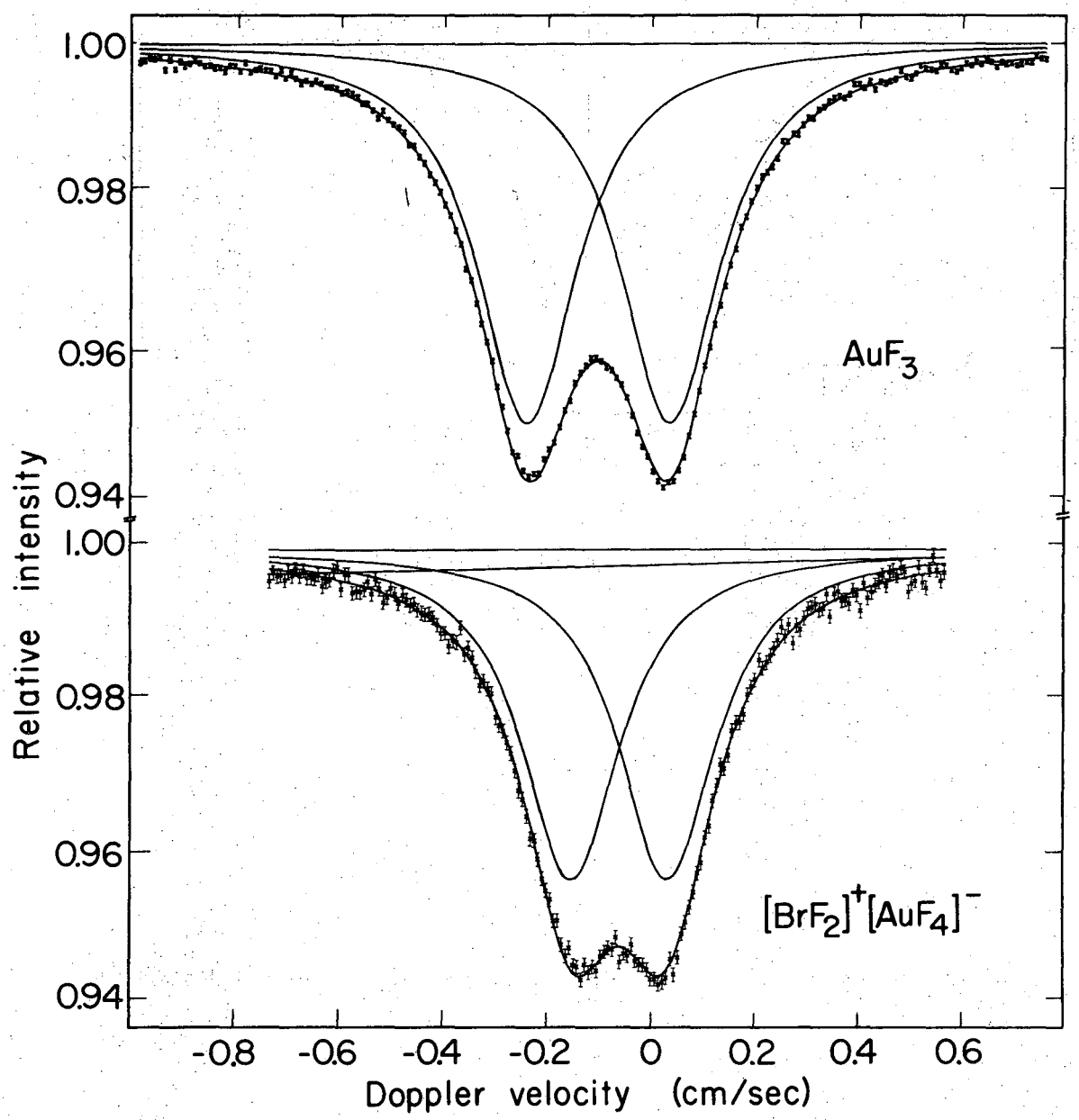

XBL694-2373

Fig. 10.

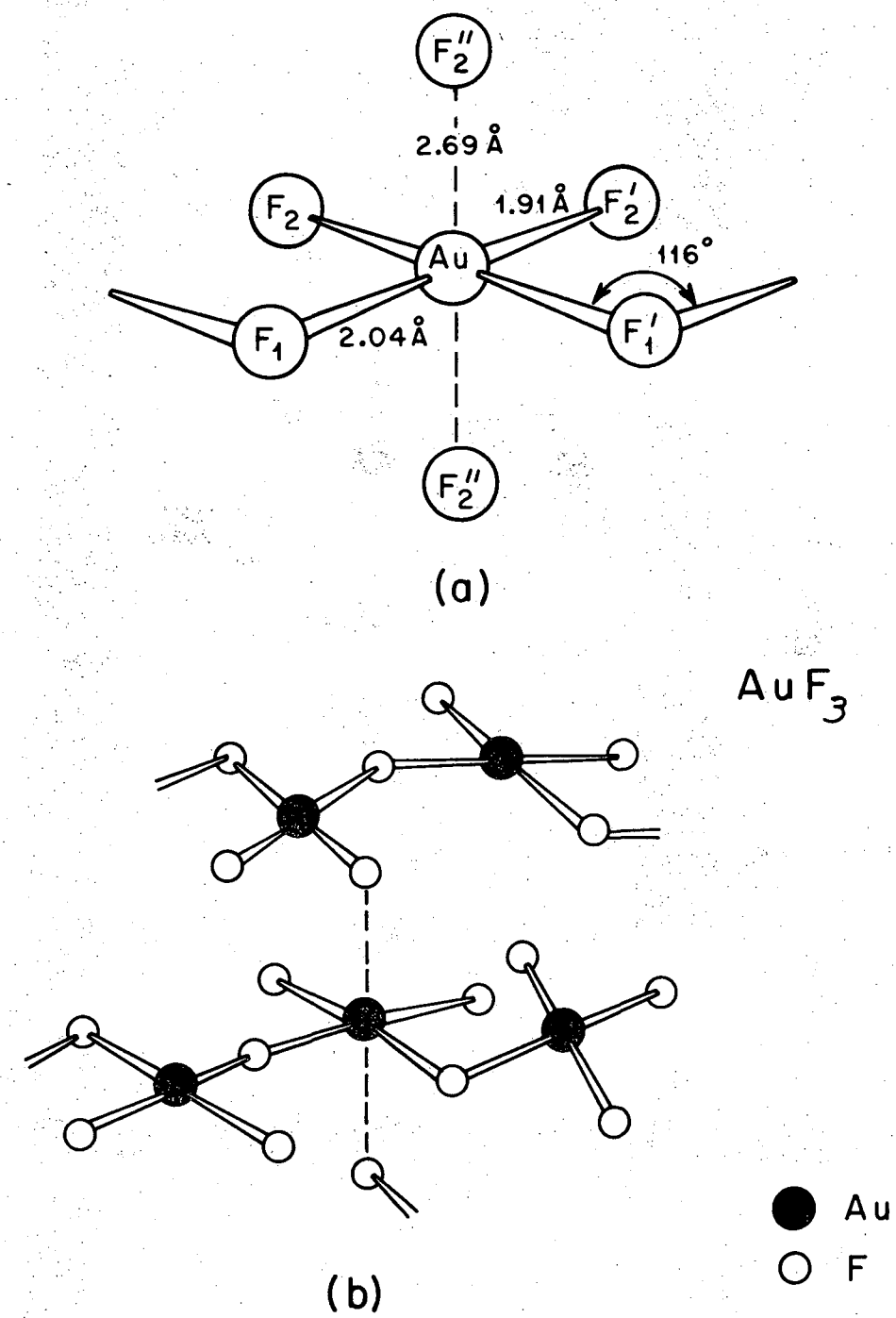

Fig. 11.

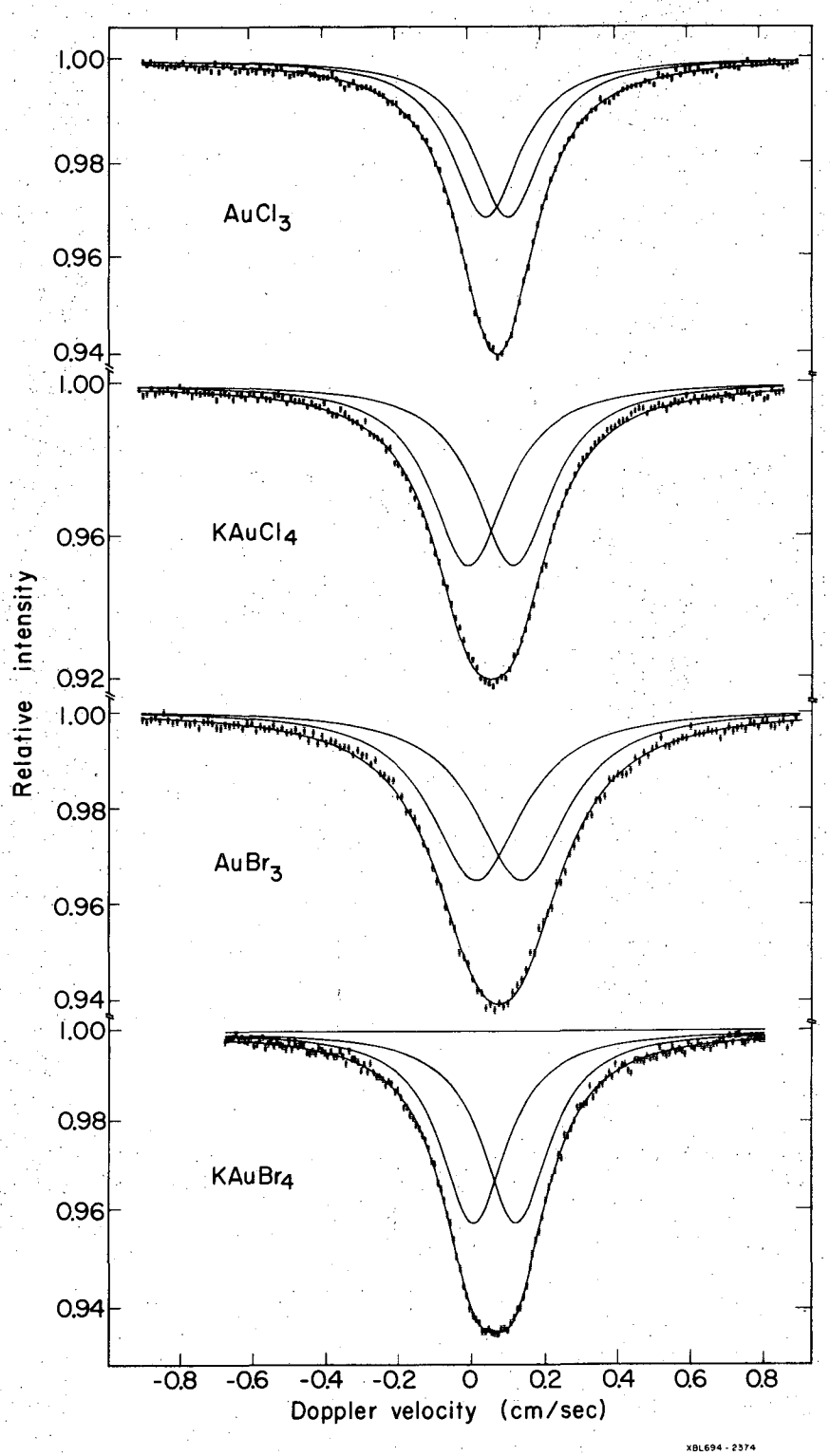
1.00
0.98
0.96
0.94
AuCl3
1.00
0.96
0.92
KAuCl4
1.00
0.98
0.96
0.94
AuBr3
1.00
0.98
0.96
0.94
KAuBr4
Relative intensity
-0.8 -0.6 -0.4 -0.2 0 0.2 0.4 0.6 0.8
Doppler velocity (cm/sec)
XBL694-2374

Fig. 12.

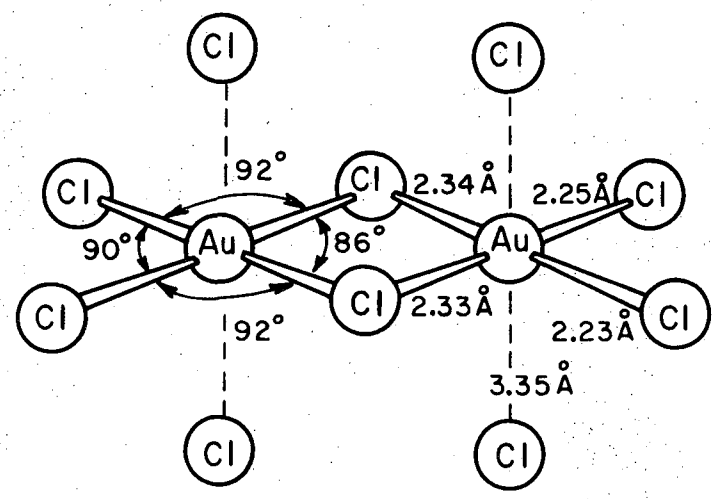
Cl
Cl
92°
Cl
Cl
2.34 Å
2.25 Å
Cl
90°
Au
86°
Au
Cl
Cl
2.33 Å
2.23 Å
Cl
92°
3.35 Å
Cl
Cl

Fig. 13.

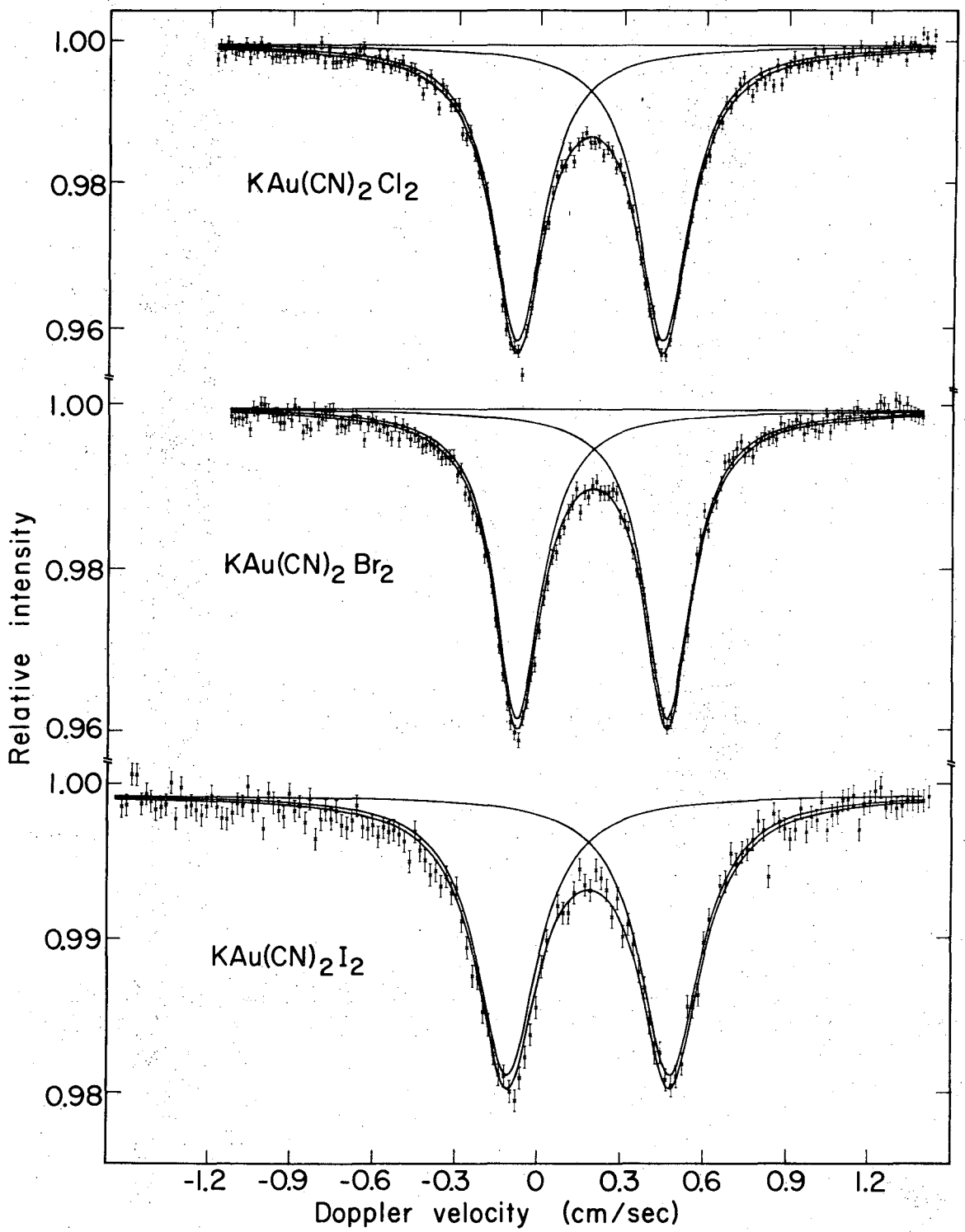

XBL694-2372

Fig. 14.

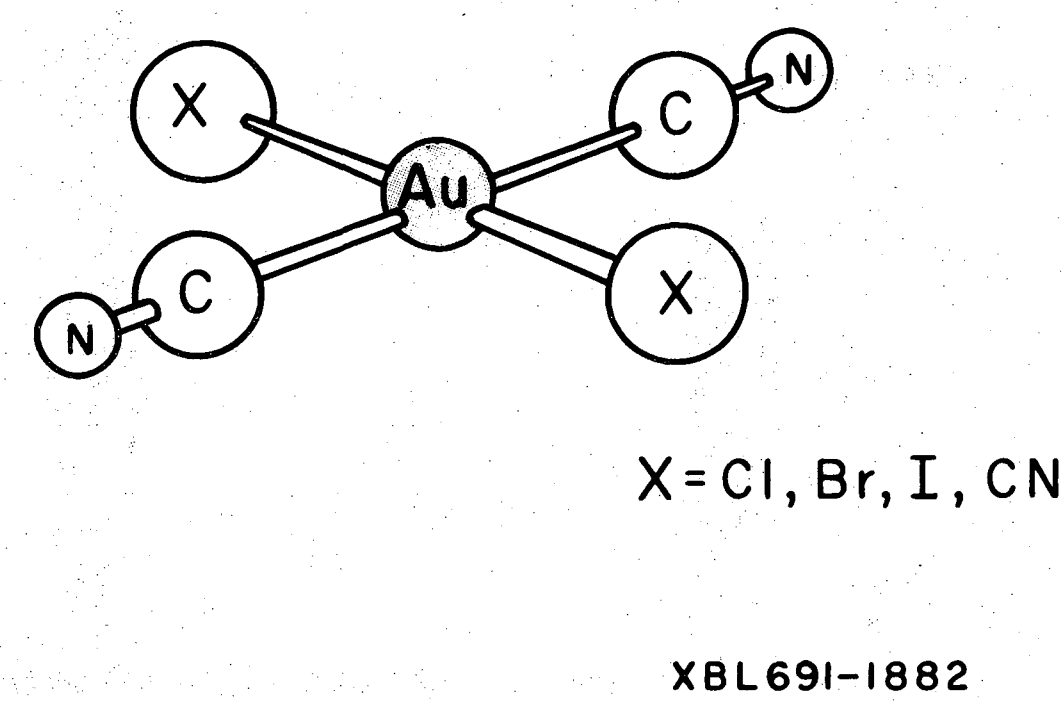

Fig. 15.

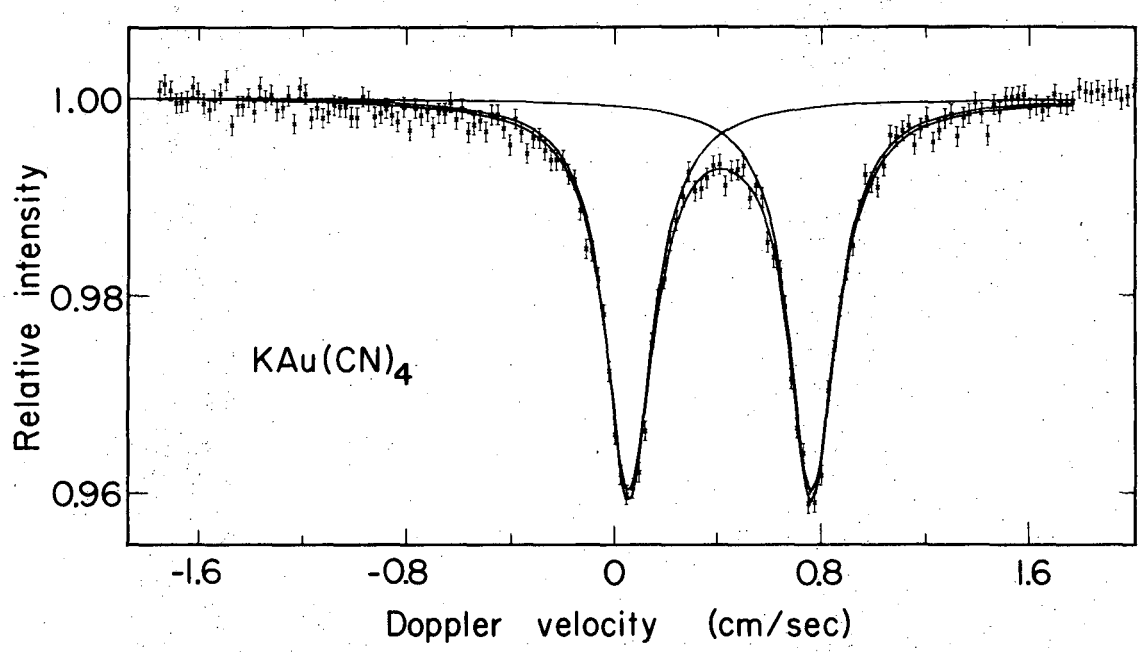

XBL694-2594

Fig. 16.

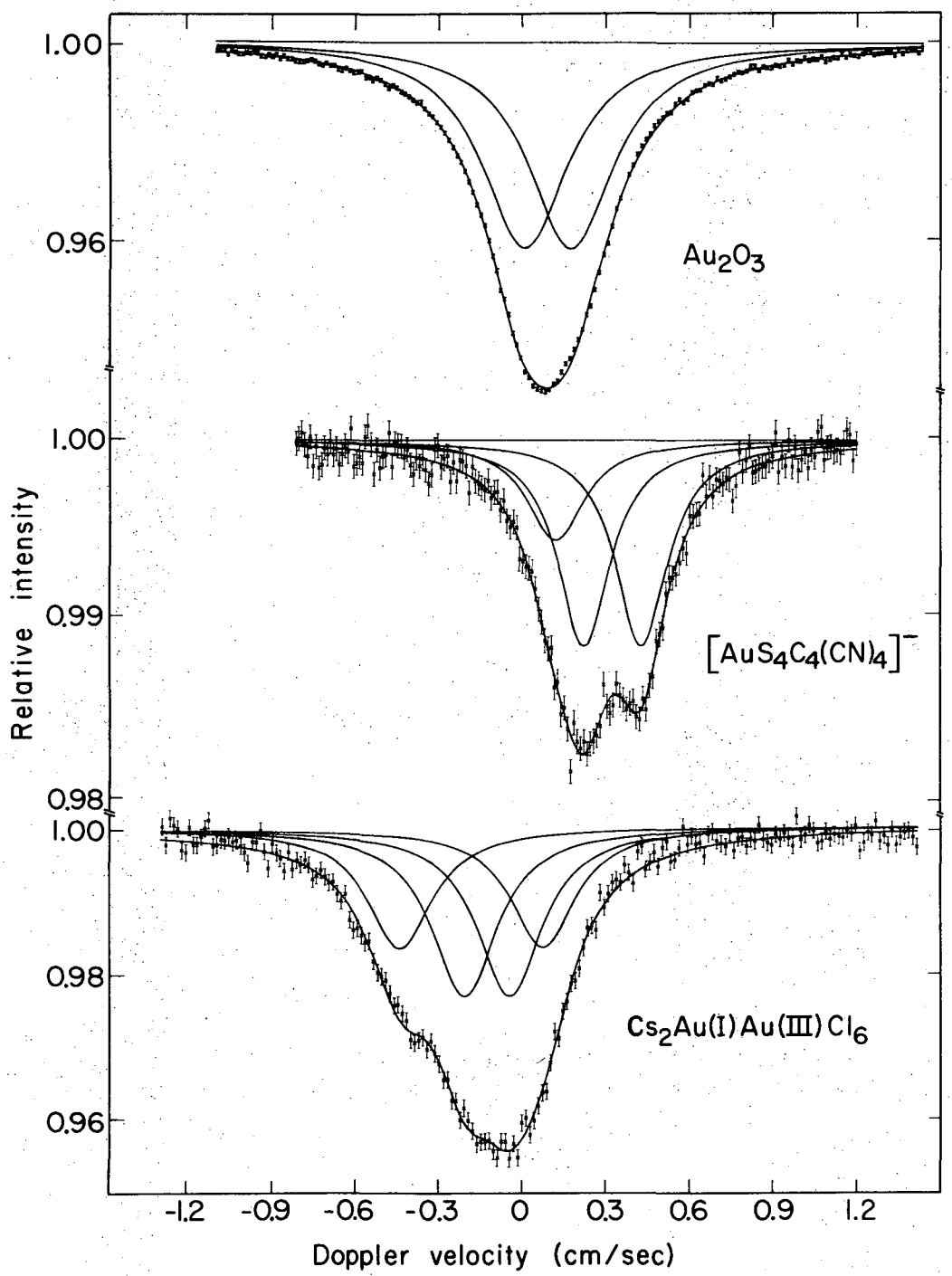
1.00
0.96
Au_2O_3
1.00
0.99
0.98
$[AuS_4C_4(CN)_4]^-$
1.00
0.98
0.96
$Cs_2Au(I)Au(III)Cl_6$
Relative intensity
-1.2
-0.9
-0.6
-0.3
0
0.3
0.6
0.9
1.2
Doppler velocity (cm/sec)
XBL694-2592

Fig. 17.

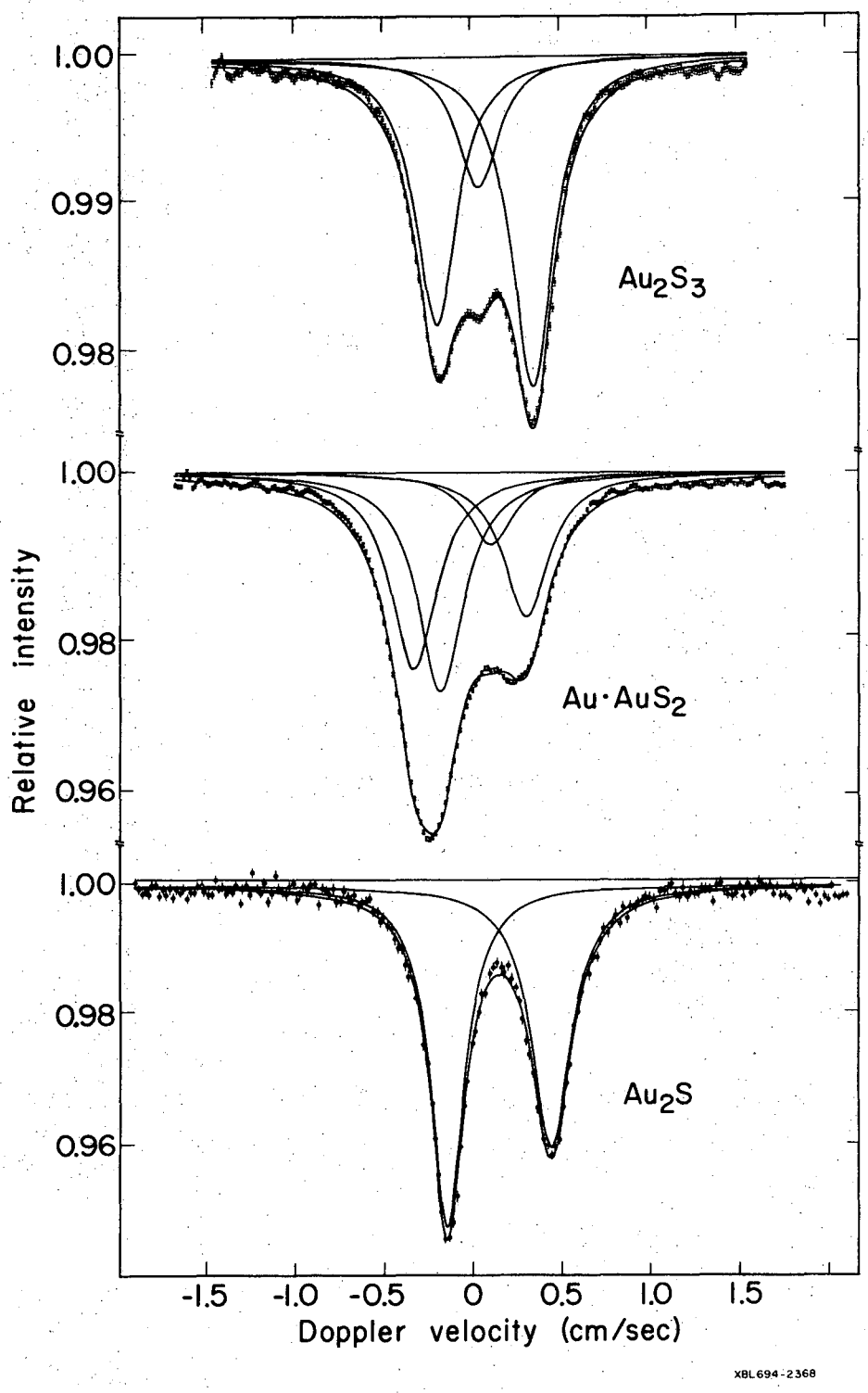
1.00
0.99
0.98
Au_2S_3
1.00
0.98
0.96
$Au \cdot AuS_2$
1.00
0.98
0.96
Au_2S
Relative intensity
-1.5
-1.0
-0.5
0
0.5
1.0
1.5
Doppler velocity (cm/sec)
XBL694-2368

Fig. 18.

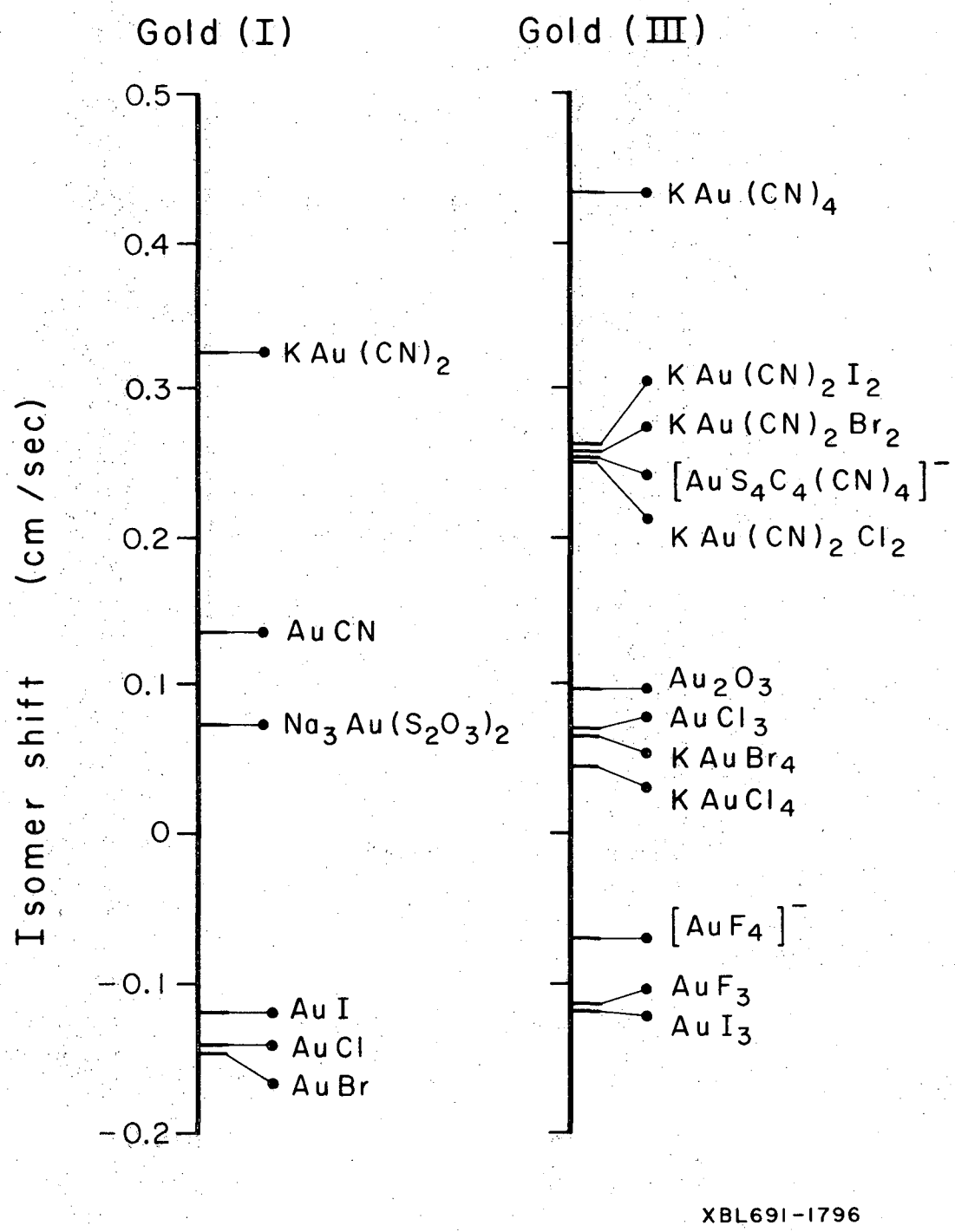
Gold (I)
Gold (III)
Isomer shift (cm/sec)
0.5
0.4
0.3
0.2
0.1
0
-0.1
-0.2
KAu(CN)2
AuCN
Na3Au(S2O3)2
AuI
AuCl
AuBr
KAu(CN)4
KAu(CN)2I2
KAu(CN)2Br2
[AuS4C4(CN)4]-
KAu(CN)2Cl2
Au2O3
AuCl3
KAuBr4
KAuCl4
[AuF4]-
AuF3
AuI3
XBL691-1796

Fig. 19.

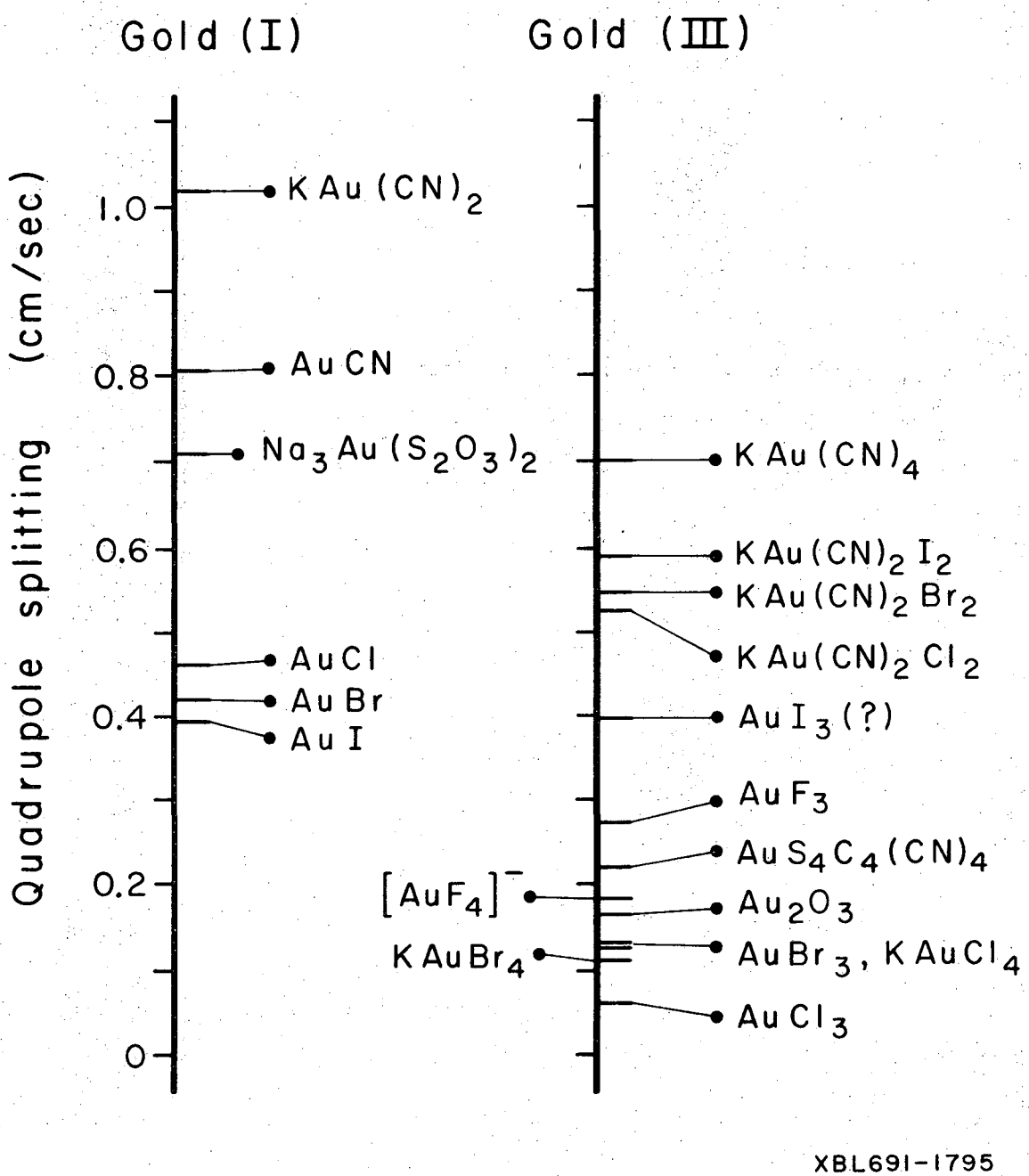
Gold (I)
Gold (III)
Quadrupole splitting (cm/sec)
1.0
0.8
0.6
0.4
0.2
0
KAu(CN)2
AuCN
Na3Au(S2O3)2
AuCl
AuBr
AuI
[AuF4]−
KAuBr4
KAu(CN)4
KAu(CN)2I2
KAu(CN)2Br2
KAu(CN)2Cl2
AuI3(?)
AuF3
AuS4C4(CN)4
Au2O3
AuBr3, KAuCl4
AuCl3
XBL691-1795

Fig. 20.

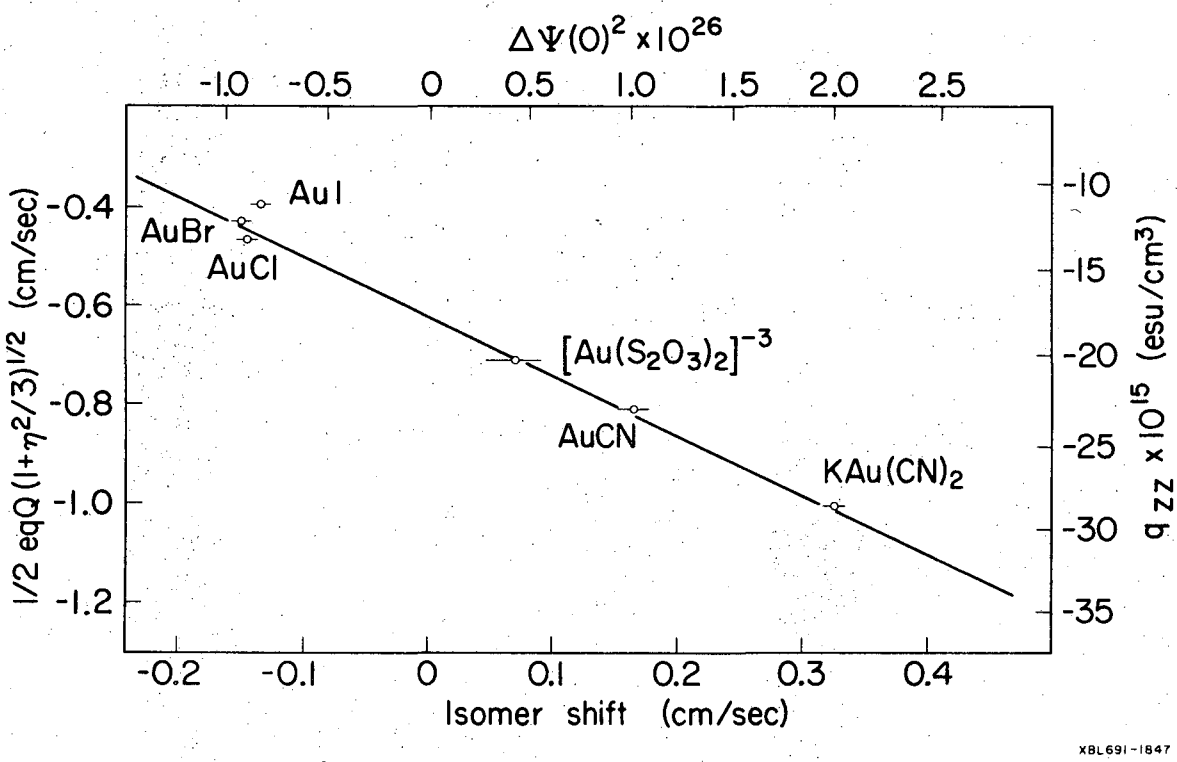
ΔΨ(0)² x 10²⁶
-1.0 -0.5 0 0.5 1.0 1.5 2.0 2.5
1/2 eqQ(1+η²/3)^1/2 (cm/sec)
-0.4 -0.6 -0.8 -1.0 -1.2
q zz x 10¹⁵ (esu/cm³)
-10 -15 -20 -25 -30 -35
AuI
AuBr
AuCl
[Au(S2O3)2]⁻³
AuCN
KAu(CN)2
-0.2 -0.1 0 0.1 0.2 0.3 0.4
Isomer shift (cm/sec)
XBL691-1847

Fig. 21.

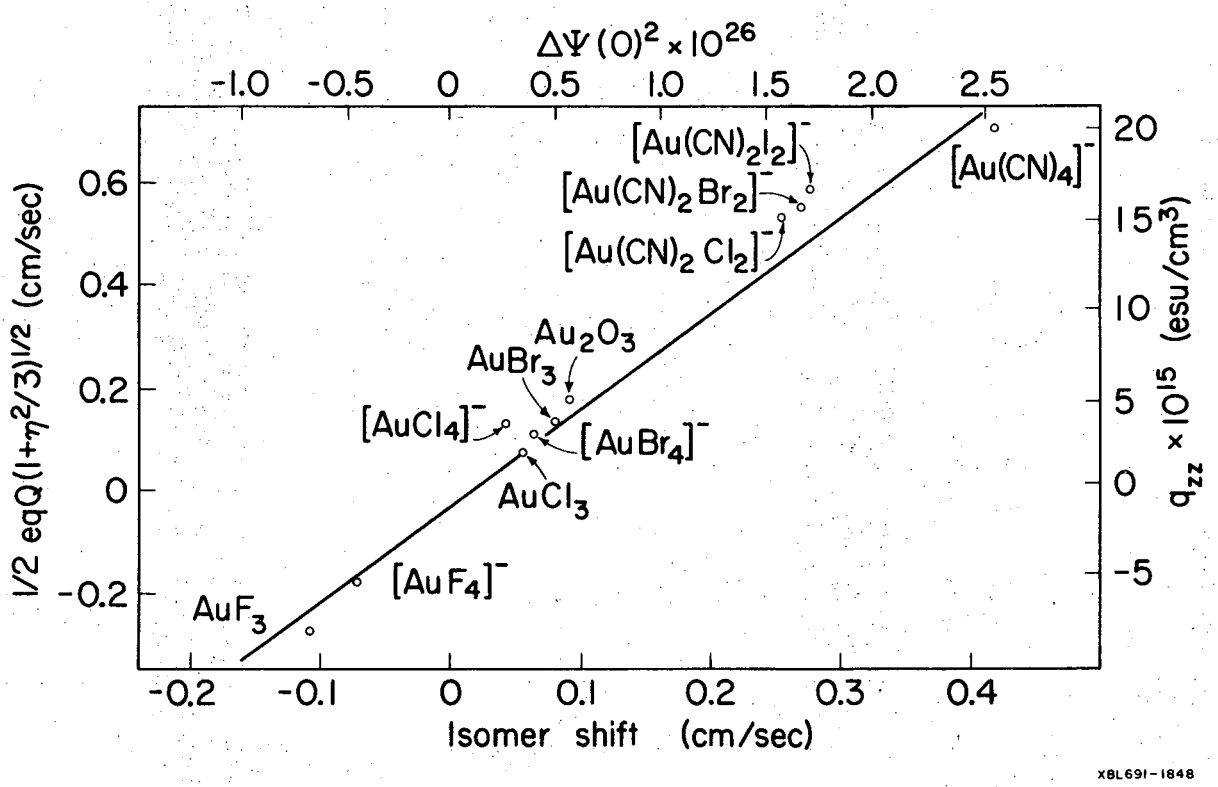
ΔΨ(0)² × 10²⁶
-1.0
-0.5
0
0.5
1.0
1.5
2.0
2.5
[Au(CN)₂I₂]⁻
[Au(CN)₂Br₂]⁻
[Au(CN)₂Cl₂]⁻
[Au(CN)₄]⁻
Au₂O₃
AuBr₃
[AuCl₄]⁻
[AuBr₄]⁻
AuCl₃
[AuF₄]⁻
AuF₃
1/2 eqQ(1+η²/3)^1/2 (cm/sec)
0.6
0.4
0.2
0
-0.2
20
15
10
5
0
-5
q_zz × 10¹⁵ (esu/cm³)
-0.2
-0.1
0
0.1
0.2
0.3
0.4
Isomer shift (cm/sec)
XBL691-1848

Fig. 22.

LEGAL NOTICE

This report was prepared as an account of Government sponsored work. Neither the United States, nor the Commission, nor any person acting on behalf of the Commission:

A. Makes any warranty or representation, expressed or implied, with respect to the accuracy, completeness, or usefulness of the information contained in this report, or that the use of any information, apparatus, method, or process disclosed in this report may not infringe privately owned rights; or

B. Assumes any liabilities with respect to the use of, or for damages resulting from the use of any information, apparatus, method, or process disclosed in this report.

As used in the above, "person acting on behalf of the Commission" includes any employee or contractor of the Commission, or employee of such contractor, to the extent that such employee or contractor of the Commission, or employee of such contractor prepares, disseminates, or provides access to, any information pursuant to his employment or contract with the Commission, or his employment with such contractor.

TECHNICAL INFORMATION DIVISION
LAWRENCE RADIATION LABORATORY
UNIVERSITY OF CALIFORNIA
BERKELEY, CALIFORNIA 94720